UNIVERSITEIT VAN PRETORIA
UNIVERSITY OF PRETORIA
YUNIBESITHI YA PRETORIA

A Novel Preparation Method For Porous Hemi-Spherical Bio-Polymeric Microparticles

Kersch Naidoo

Submitted in partial fulfilment of the requirements for the degree

MASTERS IN ENGINEERING (CHEMICAL ENGINEERING)

in the

Faculty of Engineering, Built Environment and Information Technology
University of Pretoria
Pretoria

August 2010

A novel preparation method for porous hemi-spherical bio-polymeric microparticles

Author: Kersch Naidoo
Supervisor: Dr Heidi Rolfes
Department: Chemical Engineering
Degree: Masters in Engineering (Chemical Engineering)

SYNOPSIS

A modified oil-in-water emulsion process was developed to produce novel microporous hemi-spherical polycaprolactone (PCL) microparticles called “hemi-shells”. Through the addition of a porogen such as sodium bicarbonate into the PCL-dichloromethane oil phase and emulsification in an acidic polyvinyl alcohol aqueous phase, microporous hemi-shells formed as dichloromethane evaporated. Carbon dioxide gas evolution from the porogen reaction with the acidic aqueous phase created particles with an externally microporous shell and a large internal cavity. The hemi-shells were characterized by various methods, including scanning electron microscopy and optical microscopy which were specifically used to quantify the hemi-shell yield. The final number-average particle yield of the optimised manufacturing method for particle manufacture in the 50-200 micron size range was 84%. The number-average hemi-shell yield in the same size range was 41%. These novel microparticles have potential applications in tissue engineering and drug delivery.

Keywords: Emulsion, polycaprolactone, hemi-shells, microparticles, porogen, oil-in-water, cavity, microporous, tissue engineering, drug delivery.

ACKNOWLEDGEMENTS

I would like to take this opportunity to thank the following people and organisations:

- Dr H. Rolfes (University of Pretoria) for my thesis supervision and her astute advice;
- Ms K. Easton for all her hard work on various experiments;
- Dr F.S Moolman (Council for Scientific and Industrial Research-CSIR) for his scientific dialogue;
- Dr S. van der Merwe (University of Pretoria) for his medical expertise;
- Dr R. Nilen (De Beers) for his supervision and assistance;
- Ms A. Singh (CSIR) for all her moral support and motivation.

Financial support was provided by the CSIR for this research project as well as my studies. To all those that I have not mentioned above but have played a role in their own way, my heartfelt gratitude.

TABLE OF CONTENTS

LIST OF FIGURES

LIST OF TABLES

1. Introduction

Biomaterials are defined as materials that can be used to replace, repair and augment human tissue that has been damaged through disease, trauma or normal operational wear (Hench and Erthridge, 1982). These can also be used to augment soft tissue such as in facial surgery. One such bio-polymeric material commonly employed that provides a long-term bulking effect is polycaprolactones which gradually degrade when implanted over a year or so (Hutmacher D.W, 2001).

The biomaterials research field has thus far progressed to not only providing first generation solid bio-polymeric implants such as solid polycaprolactone implants but to second generation implants that have undergone surface modification such that the implant is recognised by the body as its own and does not initiate a foreign body inflammatory reaction (Haverkorn et al., 2008).

The ultimate goal in soft tissue augmentation is however the non-synthetic route of providing tissue replacement by autologous (one's own) functional cells but the current major limitation to this approach is the lack of obtaining a large amount of functional autologous cells without causing significant injury to the patient, amongst a number of other technical issues (Klaus L, 2004). Hence, a synthetic implant that can stimulate tissue regrowth at the implantation site is the next best approach.

The currently preferred choice for synthetic implants to achieve the above aim is to incorporate a high degree of porosity into the implant thereby allowing cells to attach unto the implants either after implantation or with cells pre-cultured unto the biomaterial then implanted at the required site (Klaus L, 2004). Thus, implants with differing porosities and morphologies have been developed to regulate the cellular responses as required and to negate any inflammatory reactions (Klaus L, 2004).

In order to be as minimally invasive as possible to reduce further facial tissue

damage and possible scarring, the biomaterial needs to be able to be injected into the implantation site through a needle. This limits the size of the injectable to less than that of the needle gauge size. Typically, the needle size employed is a 21 gauge needle for which the injectable size limit is 200 micron (µm) while the lower size limit is 50µm due to lower particle sizes usually migrating from the implanted site hence resulting in a loss of bulking and in most instances, also resulting in serious side-effects (Klaus L, 2004).

The primary aim of this study was to fabricate such a uniquely shaped injectable porous implant within the above-mentioned required injectable particle size range limit for soft tissue augmentation. The envisioned unique injectable morphology was that of a hemi-spherical microporous shell that would allow for tissue bulking over the long-term yet still providing the initial bulking needed in the short-term. Compared to the conventional porous microspheres, the hemi-shell particles are postulated to allow for a greater cell loading capacity as well as allow for greater cellular nutrient and gas transfer due to the more open structure of a hemi-shell. However, proof of concept *in vitro* and *in vivo* trials still need to be conducted to verify this assumption. It is hoped that this particle design will then provide a new research direction in the augmentation field.

A novel emulsion based process was developed to fabricate the desired particles and the various factors that controlled the process were investigated to fully elucidate the mechanisms that lead to this unique morphology.

2. Literature review

The research field for this dissertation is soft tissue augmentation. Section 2.1 will elaborate a bit further on the application field. The product being developed however relates to the field of emulsions as discussed further in Section 2.2 and specifically to the field of microparticles production using emulsions as discussed in Section 2.3.

2.1 Soft Tissue Augmentation

Soft tissue augmentation refers to bulking up of certain sites of the body such as facial areas, sphincter muscles etc whereas hard tissue augmentation refers to bone and the like. The specific focus of this study is augmentation of soft tissue by a non-invasive procedure which typically means the use of a needle to deliver the bulking agent to the defect site.

There are a wide variety of biomaterials that can be used for soft tissue augmentation purposes many of which are polymeric in nature whereas for hard tissue augmentation, materials such as calcium phosphates and bioglass are commonly used. Table 1 provides a brief summary of some of the commonly used biomaterials that are used for both soft and hard tissue augmentation. Certain of these materials that are suitable for soft tissue augmentation find applications as listed in Table 2.

As can be seen in Table 1, a wide variety of materials have been used. The ultimate aim for a biomaterial that is intended for soft tissue augmentation is to restore tissue volume for the short term while restoring tissue functionality at the site of the implantation over the long term. Ultimately, one wishes to regenerate tissue by inducing ones own tissue regrowth or transplanting cells into the required site while the biomaterial degrades hence a more natural tissue replacement occurs over time restoring tissue functionality as well. A number of materials can be used hence specific criteria are needed to select a biomaterial for its intended application.

Table 1. Materials used in tissue augmentation

Materials	References
Polymer-bioglass composites	Aho et al., 2000
Collagen	Ashinof, 2000
Gelatin	Aracil et al., 1997
Teflon	Chertin et al., 2002
Silicones	Lofthouse et al., 2002
Calcium phosphates	Larsson et al., 2002
Hyaluronic acid	Lowe et al., 2001
Chitosans/chitins	Mi et al., 2002
Poly(ortho esters)	Einmahl et al., 2001

Table 2. Soft tissue augmentation applications

Applications	References
Cardia augmentation	Mason et al., 2002
Facial/Cosmetic fillers	Naoum et al., 2001
Urinary stress incontinence	Mukherjee et al., 2001
Vesicoureteral reflux treatment	Capozza et al., 2001
Faecal incontinence treatment	Kamm, 2002
Vocal fold paralysis	Courey, 2001

Table 3 lists some of the alternative treatments for soft tissue augmentation that includes the use of autologous cells. Commercially available biomaterial products in the market are listed in Table 4. With regard to existing commercial products available for soft tissue bulking, several are particularly prevalent in cosmetic applications. The resorbable tissue-derived products like collagen and cells, are characterized by the disadvantage of achieving only temporary volume filling while presenting some risk of allergic or immune response.

A number of non-invasive commercial products aimed at achievement of a permanent effect employ injectable non-resorbable polymer or polymer spheres but the materials are mostly non-bioactive (teflon, silicone, carbon-coated materials do not allow direct cell-tissue bonding to the biomaterial) so that implant migration and granuloma formation remain serious problems. Surface biocompatibility is now considered a minimum requirement for any

new product in this field (Haverkorn et al., 2008).

Table 3. Alternative therapies for soft tissue augmentation

Alternative Therapies	References
Teflon	Chertin et al., 2002
Collagen	Ashinof, 2000
Silicones	Lofthouse et al., 2002
Particulate fascia lata	Cheng et al., 2002
Micronised Alloderm	Cheng et al., 2002
Hyaluronic acid derivatives	Cheng et al., 2002
Autologous fat	Klein, 2001
Dermal fibroblasts	Berke et al., 2000
Cultured chrondrocytes	Smith et al., 2001
Bladder smooth muscle cells	Smith et al., 2001
Muscle-derived stem cells	Smith et al., 2001
Artificial inflatable sphincters	Kamm, 2002
Small intestinal submucosa	Furness et al., 2000

Table 4. Commercial products used in tissue augmentation

Commercial Products	References
Enterynx (polymer)	Mason et al., 2002
Bioplastique (silicone)	Cheng et al., 2002
Alloderm/Dermalogen (human dermal tissue)	Cheng et al., 2002
Isolagen (autologous collagen)	Cheng et al., 2002
Fibrel (porcine collagen)	Cheng et al., 2002
Dermalive (hyaluronic acid)	Bergeret-Galley et al., 2001
Restylane /Juvederm (purified hyaluronic acid)	Bergeret-Galley et al., 2001
Artecoll (polymeric microspheres)	Cheng et al., 2002
Hylan-B-gel (hyaluronic acid gel)	Wall et al., 2002
Deflux (sodium hyaluronan)	Capozza et al., 2001
Zyderm (bovine collagen)	Klein, 2001
Goretex (teflon)	Wall et al., 2002
Durasphere (carbon coated particles)	Pannek et al., 2001

Once implanted, such permanent materials are difficult to nearly impossible to remove surgically especially if complications arise. An example is that of injectable silicone, whereby complications of disfigurement and scarring can be present many years after implantation (Klaus L, 2004). Another permanent

implant presently available is Artecoll (polymethylmethacrylate microparticles suspended in bovine collagen) but this also faces certain of the issues described above coupled with the allergenicity concerns of bovine collagen requiring skin testing prior to implantation (Dmochowski et al., 2000).

This study will focus on addressing the above issues and also lead to the development of a novel microparticle structure that would allow for tissue ingrowth due to its large open cavity. The desired site for augmentation was the lower esophageal sphincter (LES) muscle for treatment of gastro-oesophageal reflux disease (GERD). The delivery to this site would be via an endoscopic needle to ensure that the procedure is minimally invasive and to reduce treatment time and cost. This limits the size of the injectable to less than that of the needle gauge size and typically, the needle size used is a 21 gauge needle for which the injectable size limit is thus between 50-200µm as previously mentioned.

Polycaprolactones (PCL), a biodegradable polyester, was selected as the biomaterial of choice for this study due to its resorbability as well as long *in vivo* degradation period of nearly a year or more (Hutmacher D.W, 2001). The resorbable nature of the biomaterial selected allows for tissue ingrowth consequently providing a persistent tissue volume effect. Due to the expected tissue ingrowth, migration of the particles from the implantation site should not occur.

It is known that the degradation products of most biodegradable polyesters result in acidic by-products which could then damage or kill cells near the implantation site due to the localised drop in pH. Polycaprolactones effectively circumvent this issue due its much smaller pH drop when degrading. Also, as a result of the highly crystalline nature of this biopolymer, mechanical strength should be retained even with a high degree of porosity. It should be noted however that clinical trials are beyond the scope of this study to verify the above hypotheses and only product fabrication and the various production factors influencing the fabrication of the product will be discussed in more detail.

2.2 Emulsions

An emulsion is the result of two immiscible components being mixed together to form a homogenous solution in which one component is distributed in the form of droplets into the other such as an oil in water emulsion (Fox C et al., 1986 & Lissant K.J. et al., 1974). The commingling of these two immiscible phases results in an increase in the interfacial area between the immiscible phases (Lissant K.J Part 1, 1974).

An emulsion typically requires stabilisation which is accomplished by the addition of a surfactant. The function of the surfactant is to lower the interfacial tension between the two components resulting in the formation of a stable homogenous solution that should preferably not separate with time (Lissant J.K, Part 2, 1974 & Part 3, 1984). Therefore an emulsion will consist of a hydrophobic phase, a hydrophilic phase and a surfactant. There are three classes of emulsions i.e. macroemulsions, nanoemulsions and microemulsions. These respective classes differ in their droplet sizes, formation and thermodynamic terms.

The droplet size in a macroemulsion is generally greater than 1µm. In a nanoemulsion, the droplet size typically ranges from 50nm to 200nm while in a microemulsion, it occurs between 10nm to 100nm (Simmonet et al., 2000 & Paolino et al., 2002). Nanoemulsions unlike microemulsions are only kinetically stable (Tadros et al., 2004). The kinetics of the emulsion formation is shown in the thermodynamic equation below (Reiss J.G et al., 2001):

$$\Delta G_{form} = \Delta A\sigma - T\Delta S_{config} \quad \text{..... (1)}$$

Where ΔG_{form} = Change in Gibbs free energy of the emulsion (J/mol)

ΔA = Change in surface area with interface creation (m^2/mol)

σ = Interfacial tension (N/m)

T = System temperature (K)

ΔS_{config} = Change in configuration entropy (J/mol.K)

The Gibbs free energy of an emulsion is a measure of the spontaneity of emulsion formation. When a low interfacial tension is reached between the two phases, a microemulsion is spontaneously formed i.e. does not require stirring and is thermodynamically stable (Rosano & Clausse, 1987). This is as a result of the use of a very high surfactant concentration and co-surfactant whereas macroemulsions and nanoemulsions only typically make use of a surfactant and requires energy. Large amounts of energy besides the high surfactant concentrations are required for smaller droplet sizes such as in the case of nanoemulsions (Tadros et al., 2004).

The Gibbs energy of a macroemulsion is positive due to the lower surfactant concentration used in comparison to microemulsions hence requiring additional energy input such as stirring for driving emulsion formation. This positive Gibbs energy of the system also means that macroemulsions are thermodynamically unstable.

2.3 Microporous Polymeric Microspheres Production

Microporous polymeric microspheres have been fabricated by many methods for a wide range of applications. Typical manufacturing methods include modified emulsion-solvent evaporation systems (Kim et al., 2006 & Edwards et al., 1997), phase separation (Hong et al., 2005), emulsion polymerisation (Hong et al., 2005) and spinning disk atomisation (Senuma et al., 2000). The most commonly used route for manufacture however still remains the emulsion-solvent evaporation technique (Hong et al., 2005).

A conventional emulsion process involves dissolving a polymer in a volatile organic solvent and emulsifying this phase in an aqueous phase containing a surfactant to form an oil-in-water (O/W) emulsion, followed by solvent evaporation while stirring. By this emulsification process, non-porous microparticles are generally obtained. However by controlling the solvent evaporation rate, for example, particles can be modified to be microporous and/or hollow (Jeyanthi et al., 1996).

To further increase the particle's porosity, porogens such as sodium chloride and ammonium bicarbonate may be added (Kim et al., 2006 & Senuma et al., 2000). The low density and high degree of porosity of the microparticles obtained by this technique makes them attractive for tissue engineering applications (Kim et al., 2006 & Senuma et al., 2000) and for pulmonary drug delivery (Edwards et al., 1997).

The oil-in-water emulsion method is suitable for the manufacture of particles of controlled size distribution combined with controlled surface morphologies. Particle manufacture by using this method is only feasible when the polymer is insoluble in water but is soluble in solvents that have partial water solubility. Alternatively, solvents that are not water-soluble but that can be removed purely through evaporation (if they have a high enough vapour pressure) can be used.

Dichloromethane is widely used for producing microspheres by the solvent evaporation method (Bittner et al., 1998). This solvent is highly volatile thus providing quick solvent evaporation for removal yet is also a very good solvent for PCL.

The surfactant dissolved in the water phase also plays a crucial role. It is needed to prevent coalescence and aggregates to form while also allowing for easy breakup of the oil droplets due to the lower interfacial tension between the oil and water phases. One of the most commonly used surfactants for oil in water emulsions is polyvinyl alcohol (Sah et al., 2000). This has gained acceptance due to other commercially available particulates using it as well. For this reason no other surfactants were investigated in this study.

During the oil-in-water emulsification procedure, with the polymer and porogen dissolved in the oil phase (Figure 1), solvent evaporation will occur over time. This will cause the polymer oil droplets to harden due to the loss of solvent. The porogen is thus microencapsulated within the polymer matrix. This porogen can then be leached out during the course of the emulsification in the case of sugar, salt porogens etc or it can be undergo some form of

erosion afterwards such as in the case of paraffin wax spheres (Ma et al., 2003) and stearic acid porogens. For a greater amount of interconnected porosity, bicarbonates (Kim et al., 2006) are typically used as they tend to foam *in situ* or by the addition of acid. A schematic of the possible route to formation of a porous microsphere by leaching of a porogen is shown in Figure 2. In this thesis, the fabrication of novel polycaprolactone microporous hemi-spherical microparticles called "hemi-shells" utilising bicarbonate porogens are investigated.

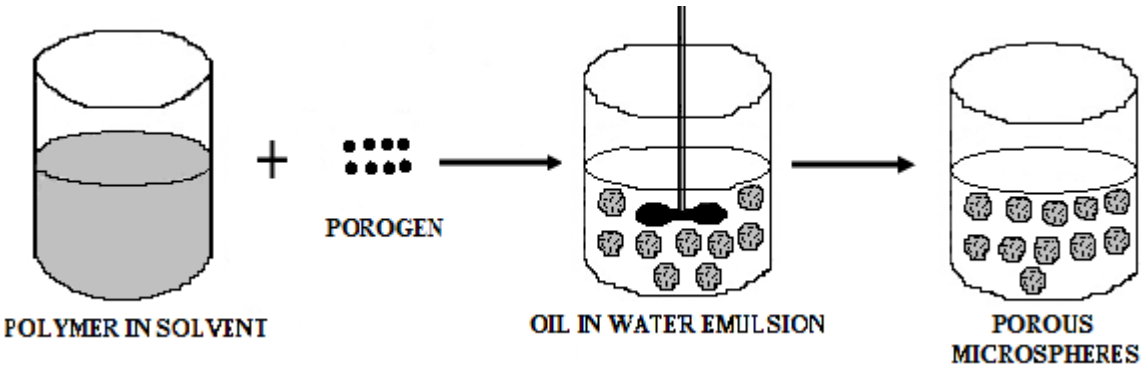

Figure 1. Diagram of an oil-in-water emulsion process for microporous particle fabrication

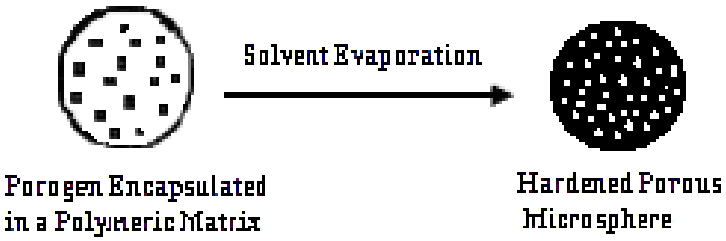

Figure 2. Schematic of porous microsphere formation

3. Materials and Methods

This chapter covers the materials that were utilised during this study as mentioned below in Section 3.1. A description of the final optimised hemi-shells method of manufacture is further elaborated in Section 3.2. Section 3.3 lists all the quantitative and qualitative methods employed in microparticles characterisation.

3.1 Materials

Polycaprolactone (CAPA 6500, Mw 50000) was purchased from Solvay Chemicals (USA). Dichloromethane (DCM), acetone and polyvinyl alcohol (PVA, average M_w 18000-23000, 87-89% hydrolyzed) reagent grade were obtained from Sigma Aldrich (South Africa) and were used as received. Glacial acetic acid (99%), sodium bicarbonate ($NaHCO_3$) and all other porogens were obtained from Merck (South Africa) and were of analytical grade. The porogens were ground down using a mortar and pestle and sieved into the required size fractions prior use. Deionised water was obtained from a Millipore water purification system. All chemicals were used without further purification.

3.2 Preparation Method For Hemi-Spherical Microparticles

PCL hemi-shells were prepared by using an oil in water (O/W) emulsion (Figure 3). PCL (15% w/v) was fully dissolved in 10ml DCM (oil phase). $NaHCO_3$ (25-38µm) was then stirred into the oil phase with a porogen: PCL ratio of 2:1 by weight. PVA (1% w/v) was dissolved in 150ml deionised water (water phase). The O/W emulsion was prepared by using a Silverson homogenizer (Model L4RT, Silverson Machines, UK) at 300rpm for 2 minutes at 25°C. The emulsion was solvent evaporated while constantly stirring at the same temperature. Glacial acetic acid (2.4ml) was added after 30 minutes to increase CO_2 gas evolution by the reaction (2), given below:

$$NaHCO_3 + CH_3COOH \rightarrow CH_3COONa + H_2O + CO_2 \uparrow \quad \text{..... (2)}$$

After solvent evaporation was completed, the hemi-shells were isolated using vacuum filtration, washed three times with deionised water and the left to dry at under a fume-hood. The final mass compositions used are shown in Figure 4.

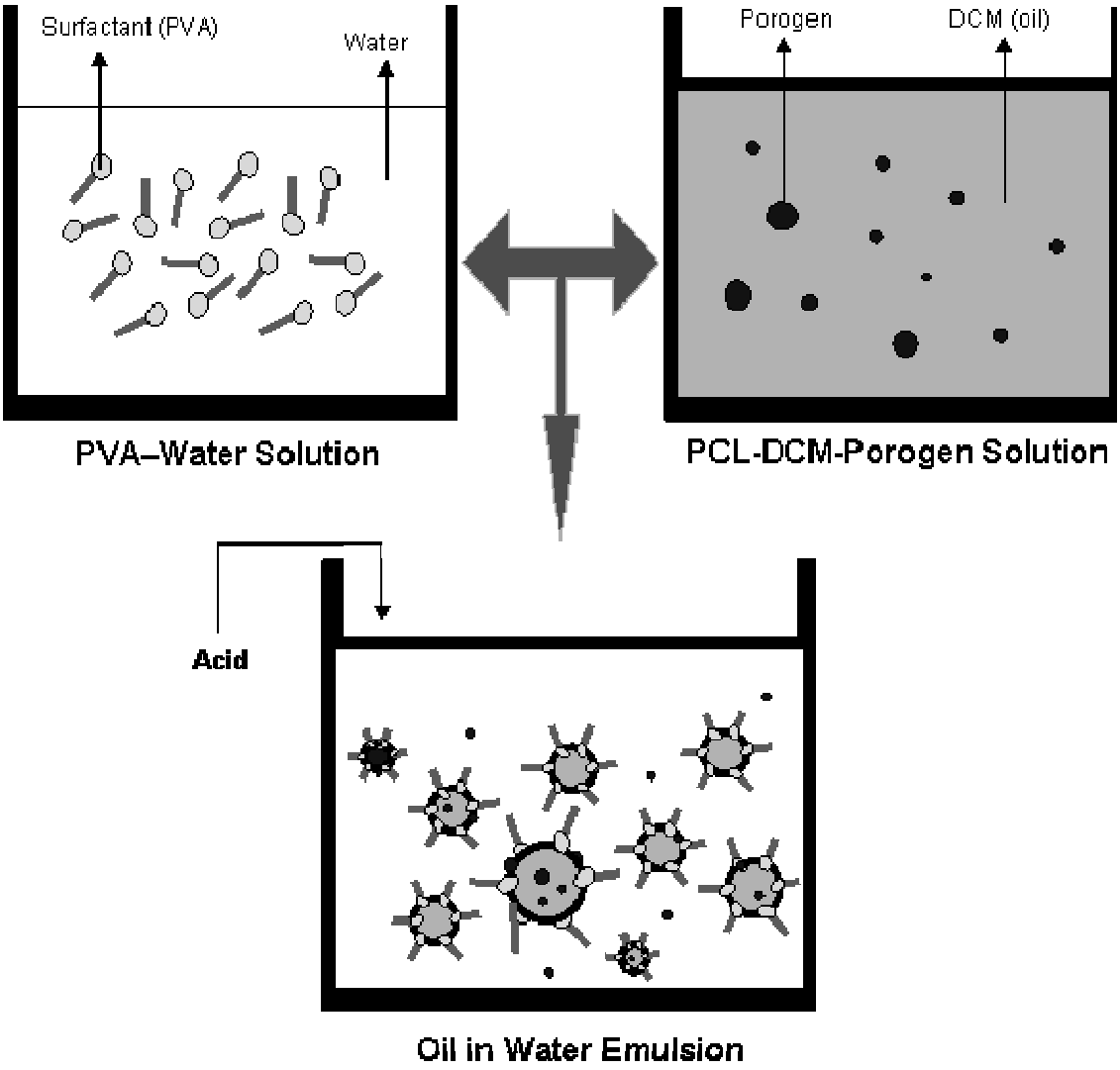

Figure 3. Pictorial overview of hemi-shells manufacture process (not drawn to scale)

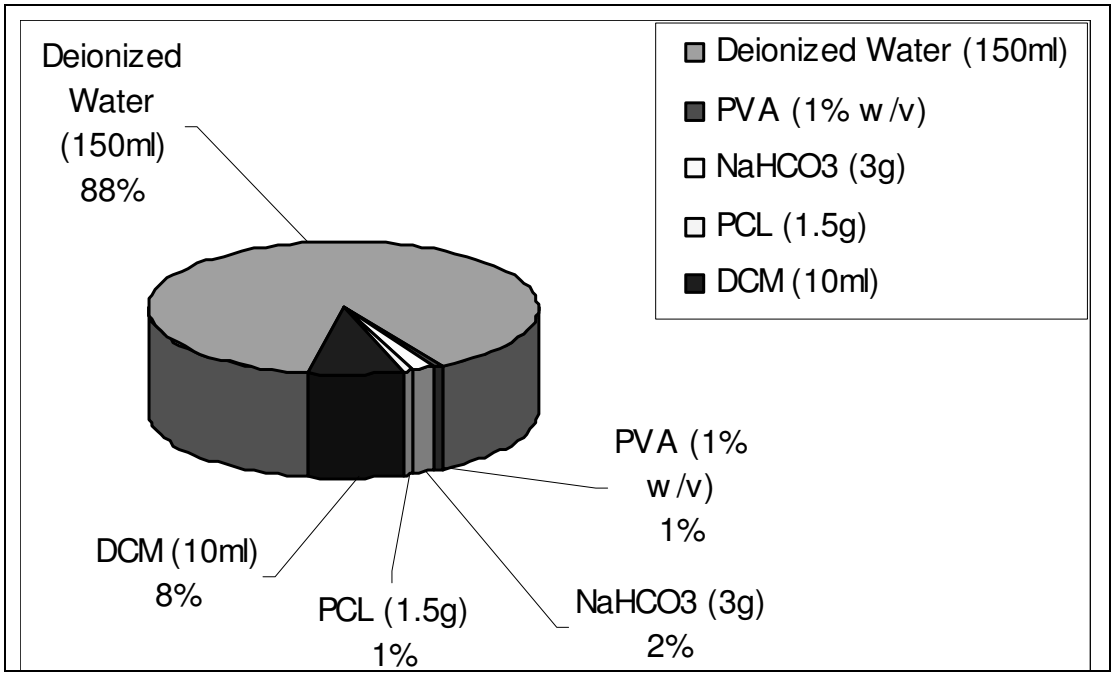

Figure 4. Mass percentage of chemicals utilised

3.3 Characterisation of Microparticles

3.3.1 Malvern Particle Size Analyser

The volume-average particle size (Dv_{50}) in microns and particle size distribution was determined using a Malvern MasterSizer 2000S laser light scattering (LLS) unit. The particle size range measurable by this unit is from 0.02µm to 2000µm. The samples were dispersed in deionised water and ultrasonicated for 2 minutes prior size analysis at 25°C.

3.3.2 Optical Microscopy

To monitor the morphological changes of the hemi-shells with time and the final particle morphology, small quantities during the emulsion process were removed at various time points as solvent evaporation advanced. These particles were then examined using an optical microscope (Leica DME, USA) with a Leica DC 150 digital camera system.

By use of image analysis software (ImageJ Vers. 1.36b, NIH), the number-average particle size (Dn_{50}) in microns and yield of hemi-shells in the injectable 100-200µm range was quantified (n = 500). Scale-bars on the optical microscope photos were obtained through calibration with stage micrometers (graticules) at the exact settings of the sample micrographs and superimposing the scale-bar on these sample micrographs.

3.3.3 Scanning Electron Microscopy (SEM)

The particle morphology was examined using a scanning electron microscope (SEM) (LEO 1525 scanning electron microscope with Oxford's INCA EDX system). The samples were mounted on conducting double-sided carbon tape and then sputter-coated with carbon prior examination. An accelerating voltage of 10kV was used. Energy dispersive spectroscopy x-ray analysis (EDX) was also performed on selected samples for surface chemical analysis.

3.3.4 Confocal Laser Scanning Microscopy (CLSM)

Confocal laser scanning microscopy (CLSM) was undertaken at University of Pretoria Microanalysis Lab using a Zeiss LSM 510M microscope equipped with a He-Ne & Argon ion laser. The images were obtained by incorporating fluorescent Nile Red (excitation λ = 550nm, emission λ = 650nm) into the PCL microparticles manufacturing process & then placing the resulting microparticles unto a clear double-sided tape. The software packages used for extracting imaging data was Zeiss LSM Image Browser Vers. 4 & ImageJ.

3.3.5 Mass, Size and Hemi-shell Yield Analysis

Mass yield analysis of all particles in the 50-200µm range were obtained using sieves with defined pore sizes. The volume-average size yield from the cumulative particle size distribution data in the above size range was obtained by subtracting the volume percent of particles less than 200µm from those less than 50µm to get the final size yield in the desired 50-200µm range.

The hemi-shells yield in the 50-200µm range was obtained by using ImageJ image analysis software and counting by eye the number of hemi-shells present per 500 particles from micrographs. There were no other known methods of sufficient accuracy from prior literature studies to undertake the hemi-shells yield analysis given the desired need to physically discern the specific microparticles morphology from the various other morphologies also present within one batch of microparticles.

3.3.6 Kruss Drop Shape Analyser (DSA)

Drop shape imaging was conducted using a Kruss Drop Shape Analyser 100S (DSA). This apparatus was used to simulate qualitatively the behaviour of the porogen in the polymer-oil phase during the emulsification process during a very short window of the initial emulsification procedures time.

3.3.7 Gas Chromatography-Mass Spectrometry (GC-MS)

Gas chromatography-mass spectrometry (GC-MS) is the typical method used to obtain residual solvent levels in polymers. Residual solvents used in biopolymeric medical devices pose a health risk. As such, since DCM is a Class 2 Food and Drug Administration (FDA) regulated chlorinated carcinogenic organic solvent, its concentration present in the hemi-shells has to be low. The maximum residual DCM level set by the FDA is 600ppm for medical devices. GC-MS has a low detection limit of up to 10ng/L for organic solvents (Mhlanga SD, 2004) hence is suitable for detection at the low levels needed.

The analysis was undertaken at University of Witwatersrand. It was performed on a GC-17A Shimadzu gas chromatographic technique equipped with a flame ionization detector (FID). The system was fitted with a Teknokroma capillary column TRB-624 (30×0.25mm×1.4µm). For analysis of dichloromethane, the operating conditions used were as follows: the column temperature was set at 60℃ for 30 min; this is the optimum temperature

programming for the best separation and run time. The inlet (or injection port) and detector temperatures were kept at 280℃. Argon was used as a carrier gas, at a constant flow rate of 20ml/min. Other than argon, hydrogen and air were used as flame gases. Sample injections used were 1µl.

4. Results and Discussion

The order of the results presented in this chapter is illustrated in Figure 5. As shown, the experimental variables investigated were separated into the respective phases that the experimental factors belonged to, such as the oil, water phase and the emulsion factors. In order to reduce the total number of experiments conducted, only the main factors that could lead to significant changes in particle size distribution and hemi-shell yield were investigated based on prior learning from the literature review conducted in Section 2.3. Due to the various potential particle morphologies as shown in Figure 6 that are obtainable, the optimal experimental factors that lead to the highest hemi-shell yield needs to be found.

Oil phase factors that were thus selectively chosen for further investigation included porogen type and size, polymer concentration and co-solvents. The water phase factors investigated were surfactant concentration and molecular weight, acid concentration, deionised water volume and emulsion temperature. The emulsion formation factors examined were the homogenizer type, speed and time and the solvent evaporation type. The results obtained are discussed further below.

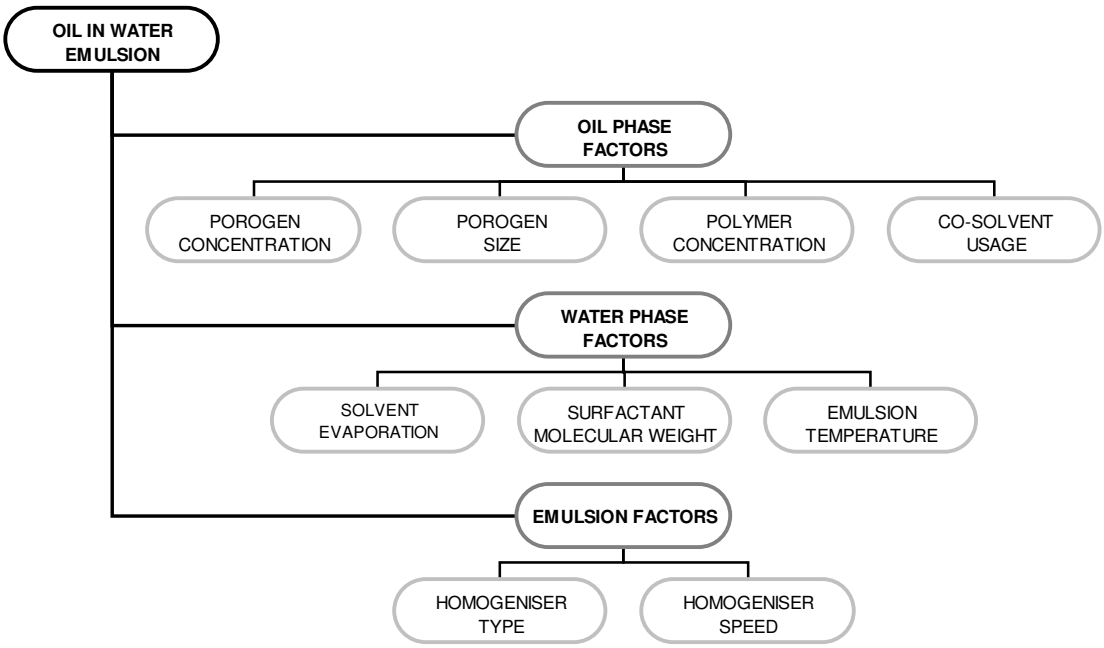

Figure 5. Experimental variable ordering

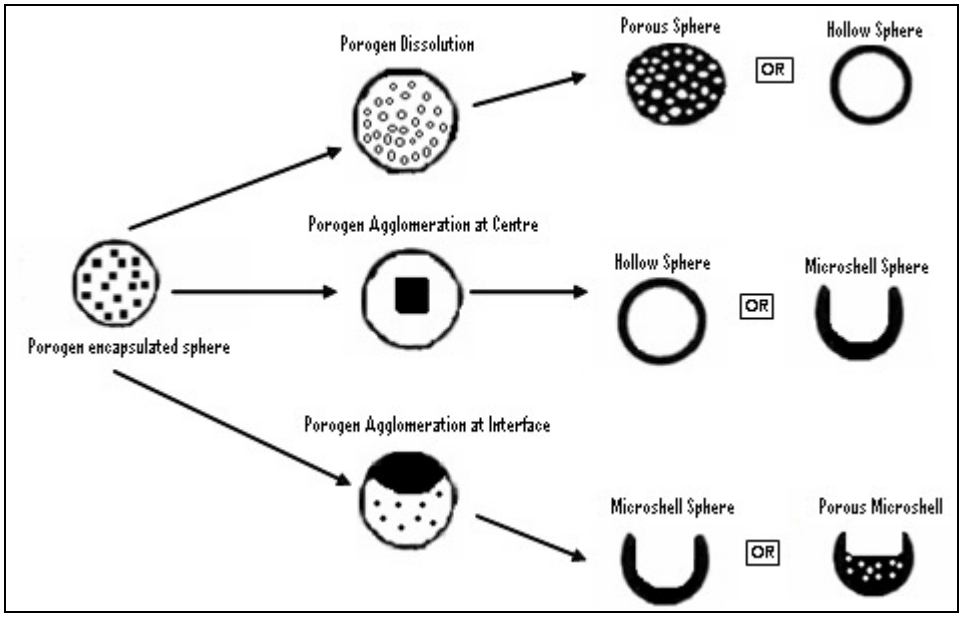

Figure 6. Schematic of various potential particle morphologies

4.1 Oil Phase Variables

4.1.1 Co-Solvent Usage

Varying amounts of a co-solvent (acetone) was co-mixed with dichloromethane (DCM) in order to reduce the amount of carcinogenic DCM and to increase the solvent evaporation time due to the higher evaporation rate of acetone compared to DCM.

The use of acetone results in an increasing volume-average size with an increasing acetone volume (Figure 7). The average particle size was seen to increase from 225µm to 310µm with an increase in acetone from 0% v/v to 50% v/v. This is possibly due to the low oil phase viscosity which results in a higher number of particle collisions hence greater droplet coalescence and so, a larger particle size (Hakkinen A et al., 2002). The particle size increase can also be attributed to the quick dissipation of acetone into the water phase resulting in quick microsphere solidification (Hong Y et al., 2005).

The volume-size, hemi-shell and mass yield in the 50-200µm range were all

seen to decrease with an increase in acetone concentration in DCM (Figure 8). The volume yield of microparticles in the desired size range was seen to decrease from 35% to about 25% with an increase in acetone addition. This result could be attributed to what was previously mentioned on quick microparticles solidification.

The decrease in hemi-shell yield to 20% with an increase in acetone volume of 50% v/v in DCM illustrated that the oil phase viscosity plays an important role in hemi-shell formation. By increasing the acetone volume percent in DCM, a lower oil phase density and viscosity is known to result (Hakkinen A et al., 2002) but it is postulated that this could then lead to an increase in porogen solubility and diffusivity in the water phase as well. This porogen loss could have resulted in the hemi-shell yield decrease observed.

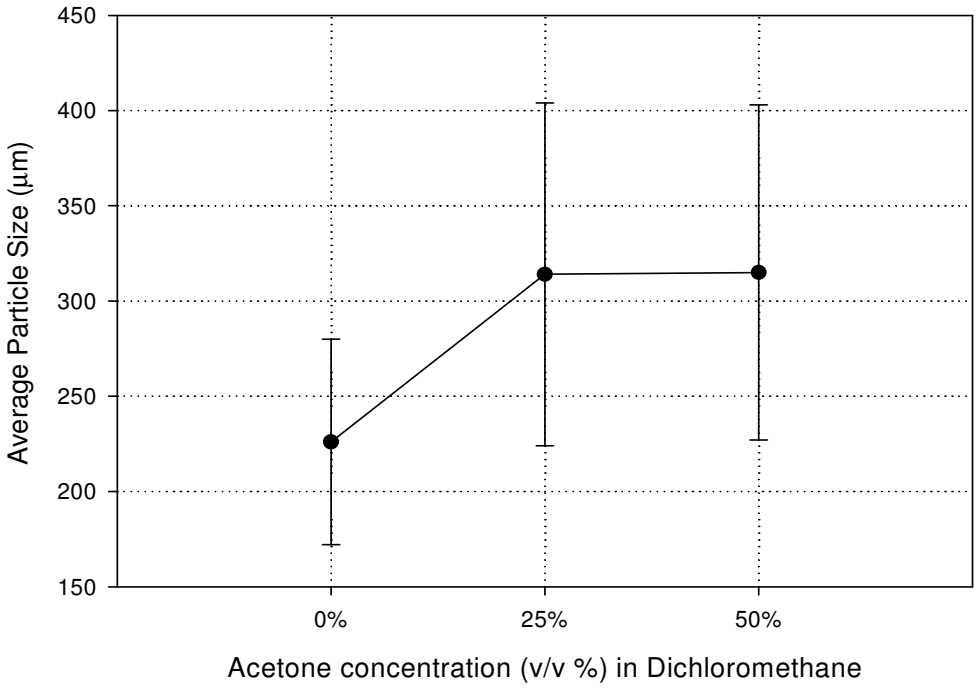

Figure 7. Effect of acetone concentration (v/v %) on the volume-average particle size (µm)

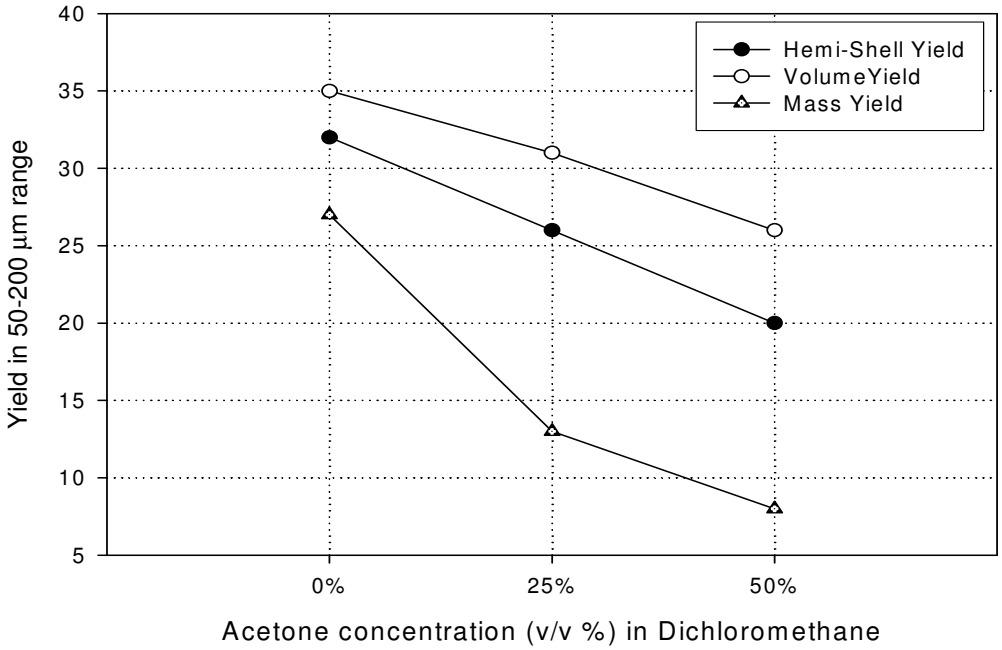

Figure 8. Effect of acetone concentration (v/v %) on hemi-shell, volume and mass yield % in the 50-200µm size range

4.1.2 Polymer Concentration

In order to achieve a higher size yield of particles in the 50-200µm range, the effect of polycaprolactone (PCL) concentration was investigated based on the effect that the oil phase viscosity had, as seen previously, on the volume-size yield. It was expected that an increase in oil phase viscosity due to the higher polymer concentration would result in larger microparticles as was similarly found by Hong Y et al (2005).

The average particle size increased from 75µm to about 225µm when the PCL concentration was increased from 0.5g to 1.5g (Figure 9). As expected, when the PCL concentration was increased three-fold, so too did the average particle size. The volume yield in the 50-200µm range was seen to decrease with an increase in polymer concentration from 80% to 52%. Due to the larger average particle size of 225µm, the volume yield of particles in the desired size range was expected to decrease. Hence, an inverse relationship between the average particle size and volume yield can be seen.

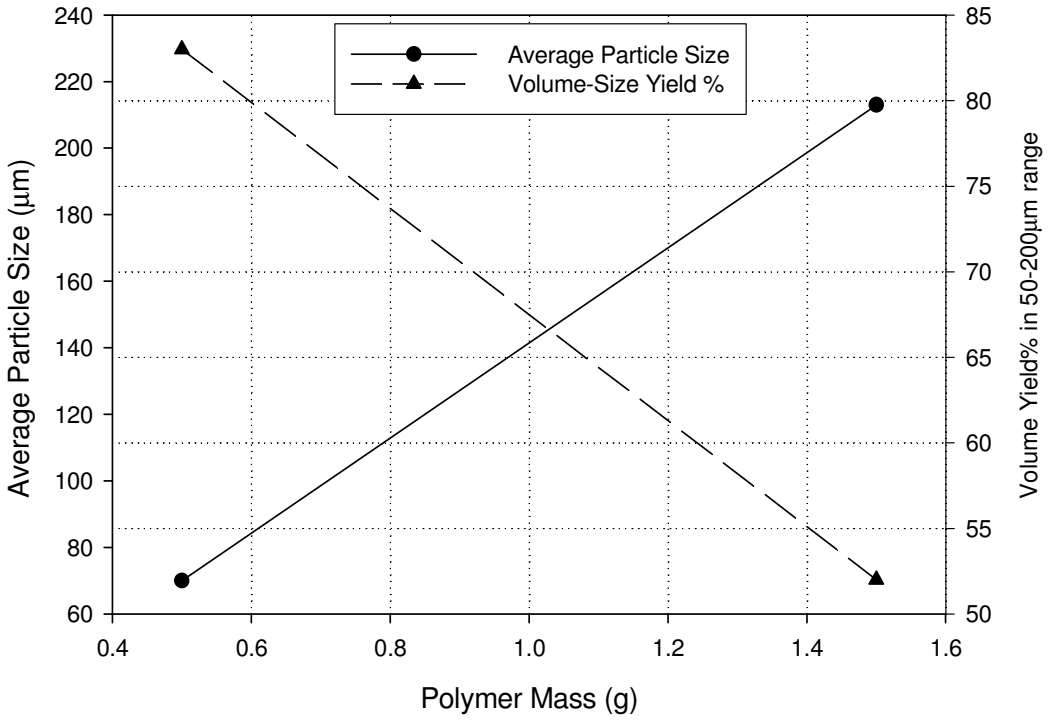

Figure 9. Effect of PCL concentration on the average microparticle size and volume yield % in the 50-200µm size range

4.1.3 Porogen Concentration

An increase in porogen concentration is known to increase porosity as well as result in an increase in the average particle size due to the increase in internal porosity (Kim et al., 2006). Figure 10 illustrates this increase in average microparticles size from 92µm to 277µm when the porogen mass was increased from 0g to 3g.

Once again, the inverse decrease in volume yield from about 93% to 32% was seen when the average particle size increased. This behaviour was attributed to the porosity increase as was observed by Kim et al (2006). SEM micrographs (Figure 11) also served to confirm this hypothesis by the qualitative increase in surface porosity as well as hemi-shell yield observed when more porogen was used. From this, it can be seen that any further increase in porogen loading above 3g will result in volume-size yields lower

than 30%. Even though an increase in hemi-shell yield would most likely occur if porogen loading was increased, an optimum porogen loading exists that will allow for the maximum volume yield and hemi-shell yield.

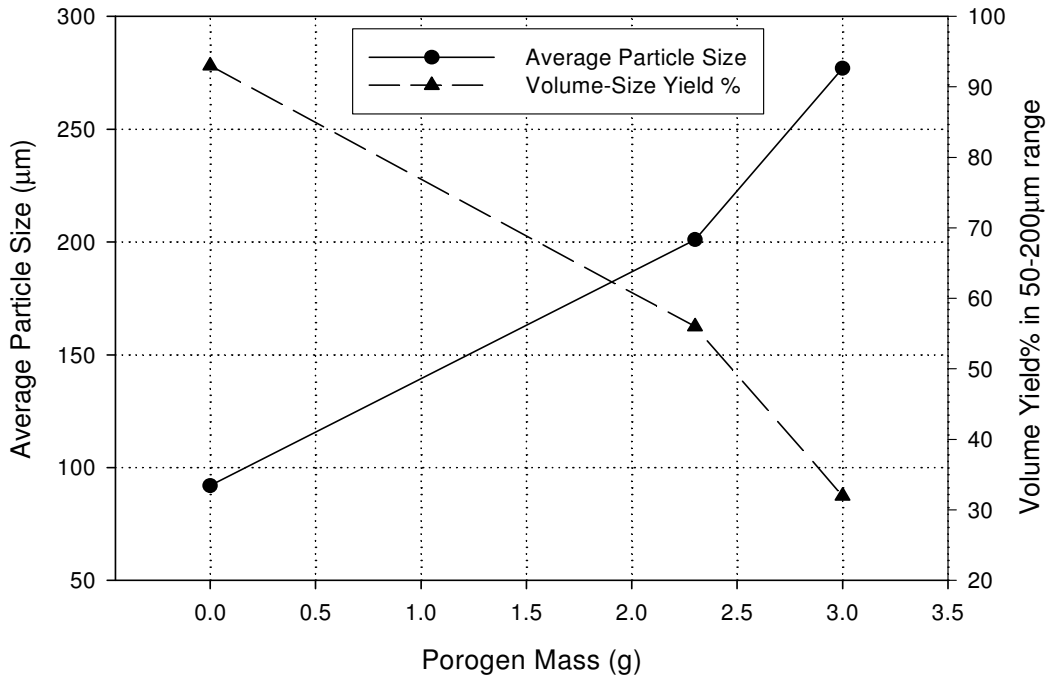

Figure 10. Effect of varying porogen size on the average microparticles size and volume yield% in the 50-200µm size range

(a)

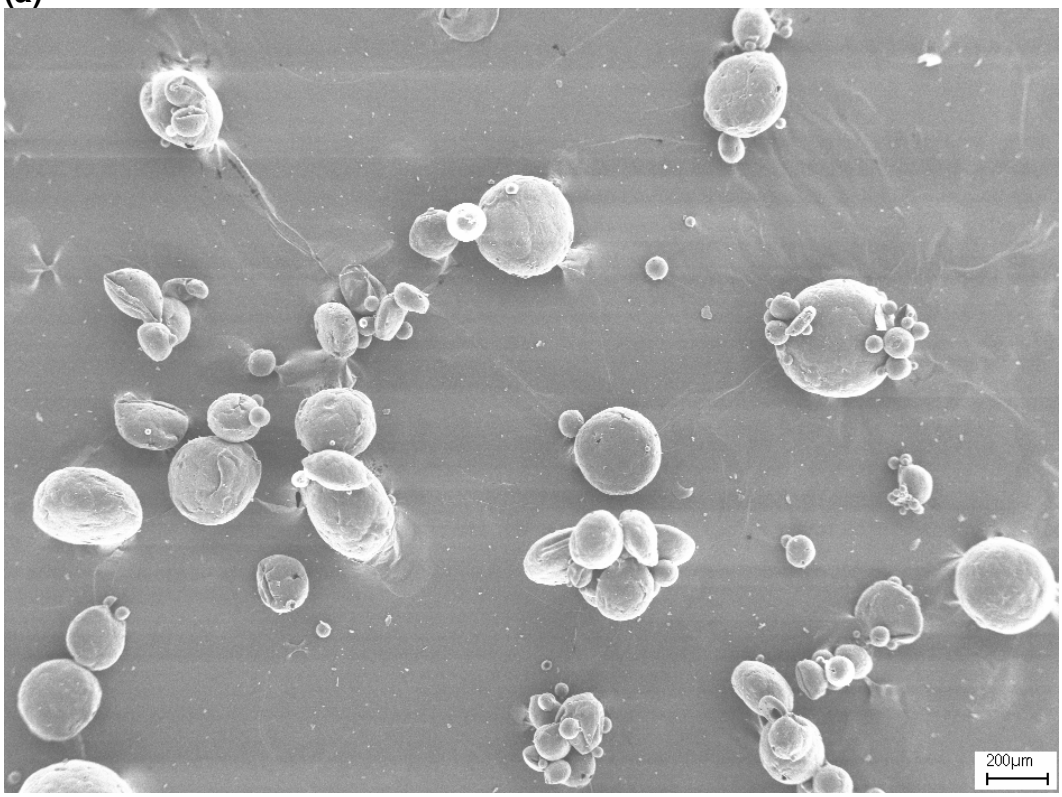

(b)

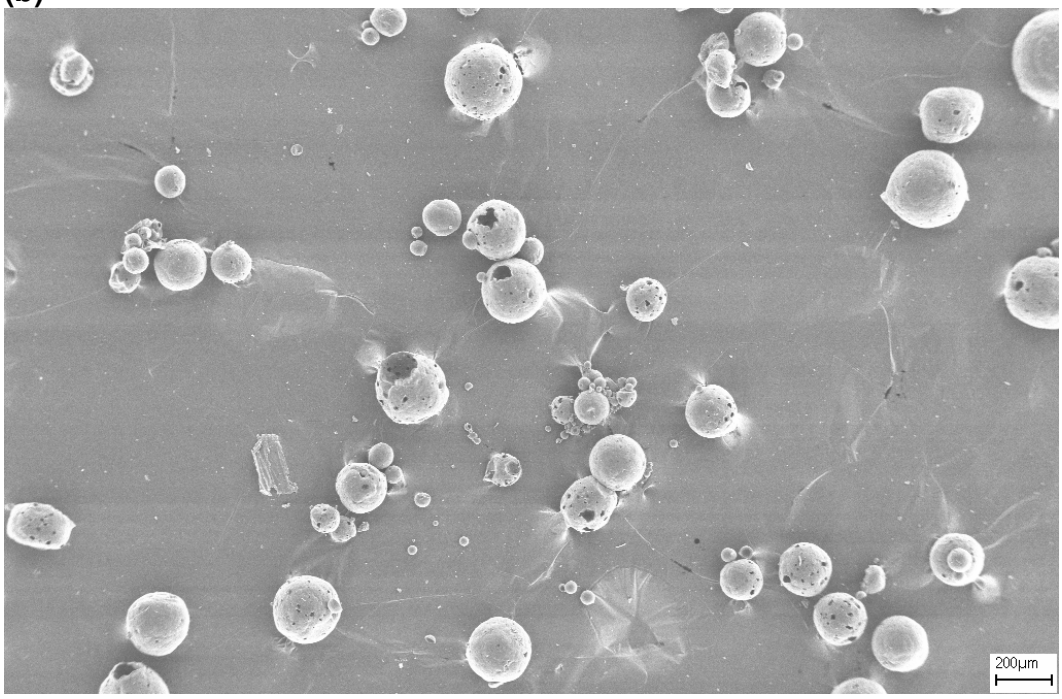

Figure 11. SEM micrographs of (a) 2.3g and (b) 3g porogen (scalebar = 200µm)

4.1.4 Porogen Size

The porogen size was also investigated as it is known from prior literature that larger porogen sizes tend to increase porosity (Noh I & Choi Y.J, 2004). Due to the polydisperse nature of the porogen, the porogen was sieved in the desired particle size range. Figure 12 illustrates the increase in average particle size from 92µm to 135µm as the average porogen size was increased from 0µm to 125µm. A larger average particle size was however noted when the smaller 32µm porogen average size fraction was used compared to the larger 125µm porogen.

The volume yield behaved as expected, inversely to the average particle size trend. The larger average particle size achieved when using a smaller porogen size did not seem to follow the conventional thinking that larger sized porogens should result in greater porosities and hence larger average particle sizes (Kim et al., 2006).

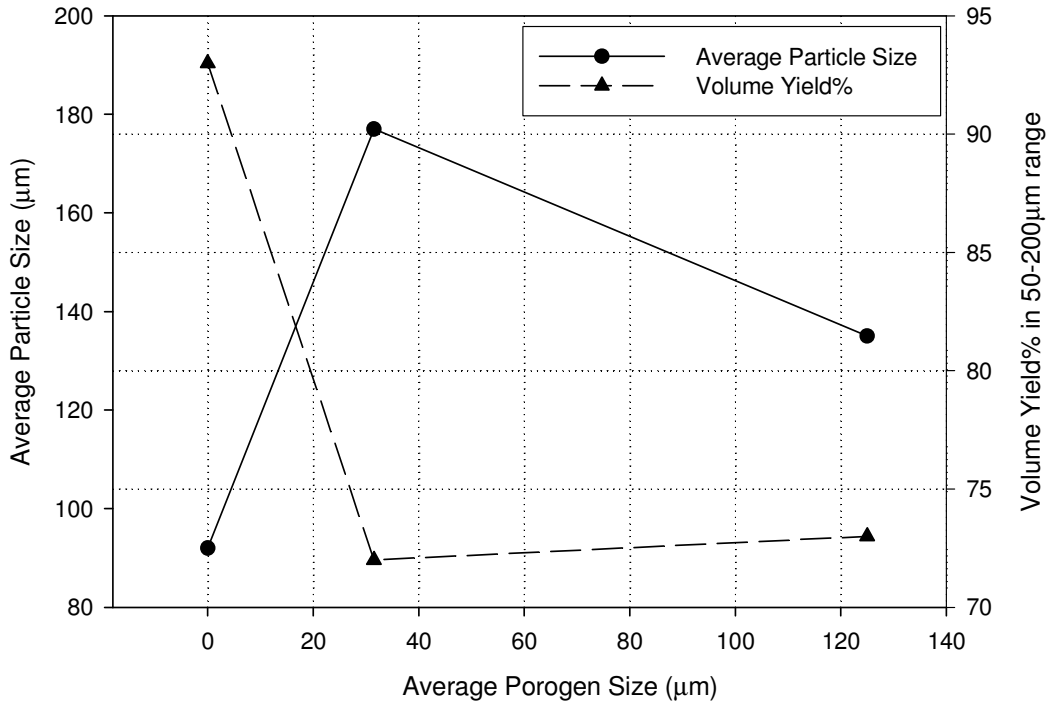

Figure 12. Effect of porogen size on the average microparticles size and volume yield% in the 50-200µm size range

To establish a reason for this unusual trend, a further experiment was conducted by simulating porogen homogenisation in an oil mixture. Figure 13(a) depicts an oil phase containing porogen prior homogenisation while 13(b) illustrates porogen sheared after homogenisation. This demonstrates that when the large porogen is homogenised, smaller porogen particles are formed due to porogen shearing.

It was postulated that this porogen size decrease results in greater number of porogen particles but with a corresponding increase in porogen loss due to dissolution in the water phase hence fewer surface pores as well as a smaller particle size. For a fixed porogen mass, the smaller sized porogen would have a greater number of particles compared to the larger porogen size fraction even with porogen shear. This hypothesis was also confirmed with SEM micrographs that showed a qualitative increase in surface porosity and hemi shell yield when smaller porogens were used compared to larger ones (Figure 14).

(a)

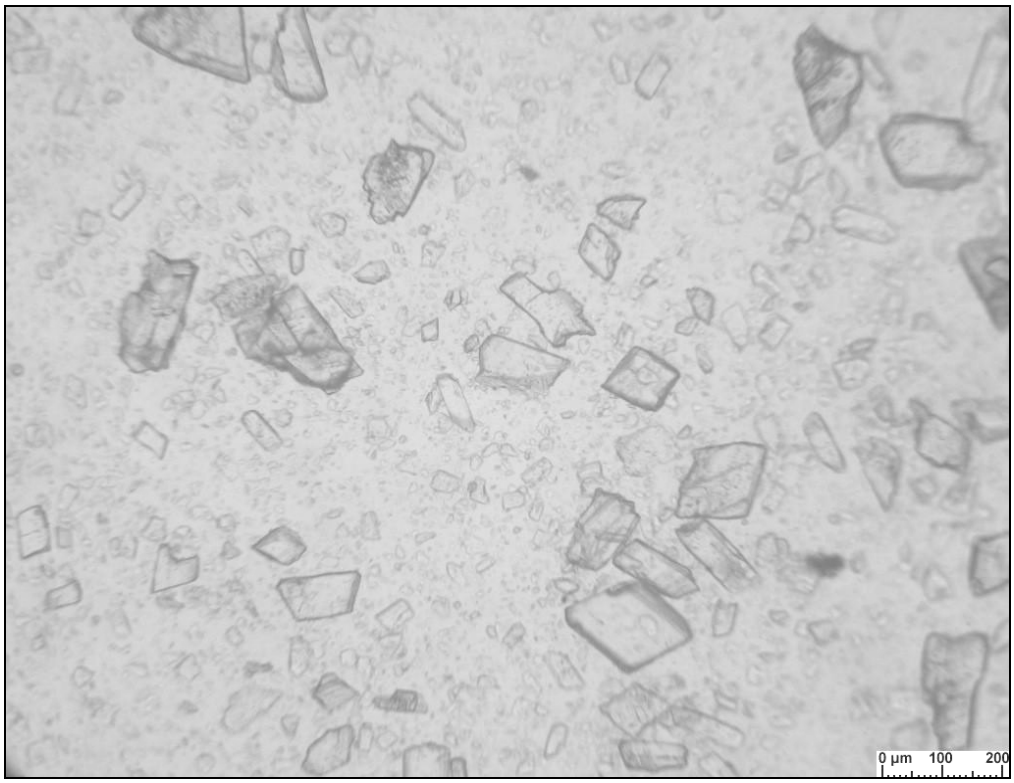

(b)

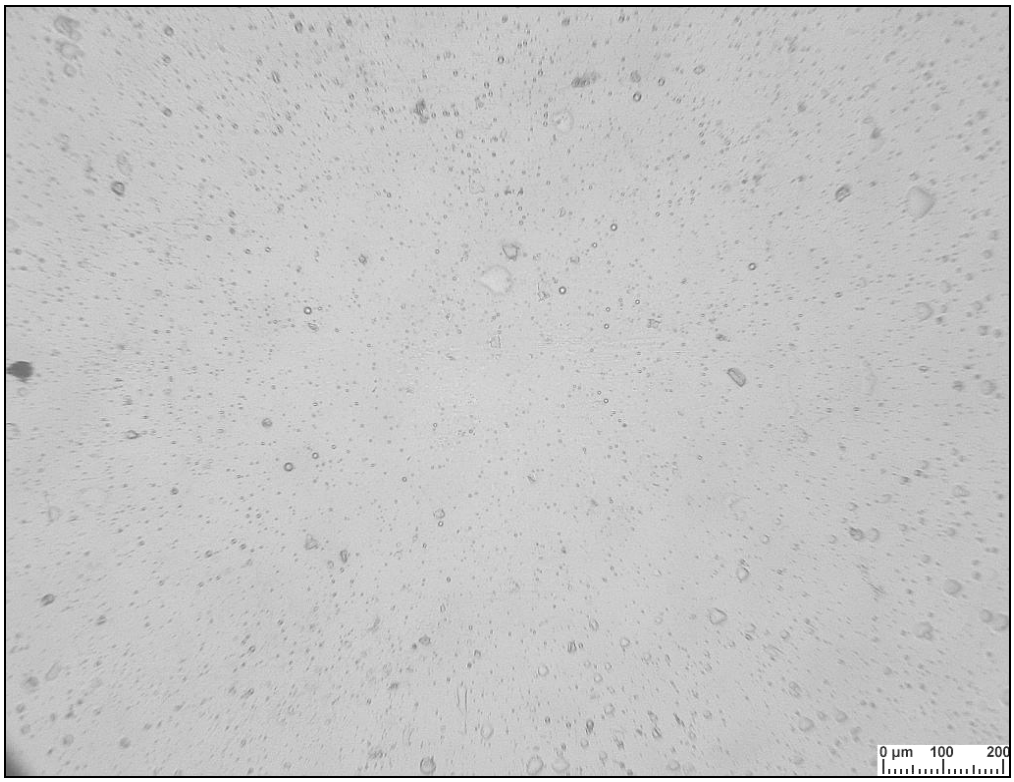

Figure 13. (a) Porogen before and (b) after homogenisation (scalebars = 200µm)

(a)

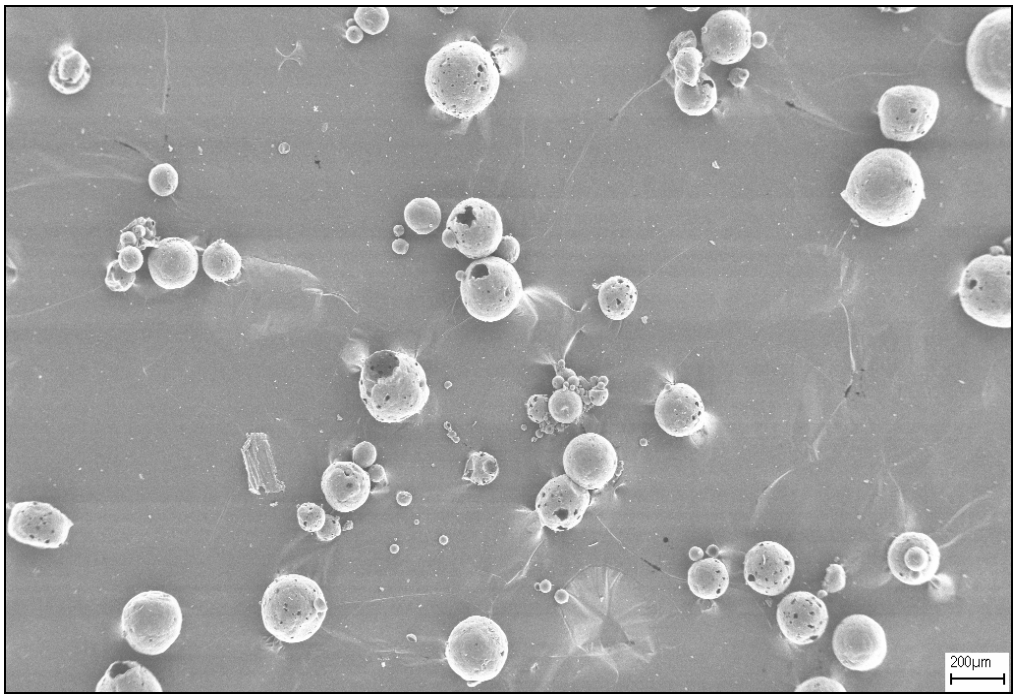

(b)

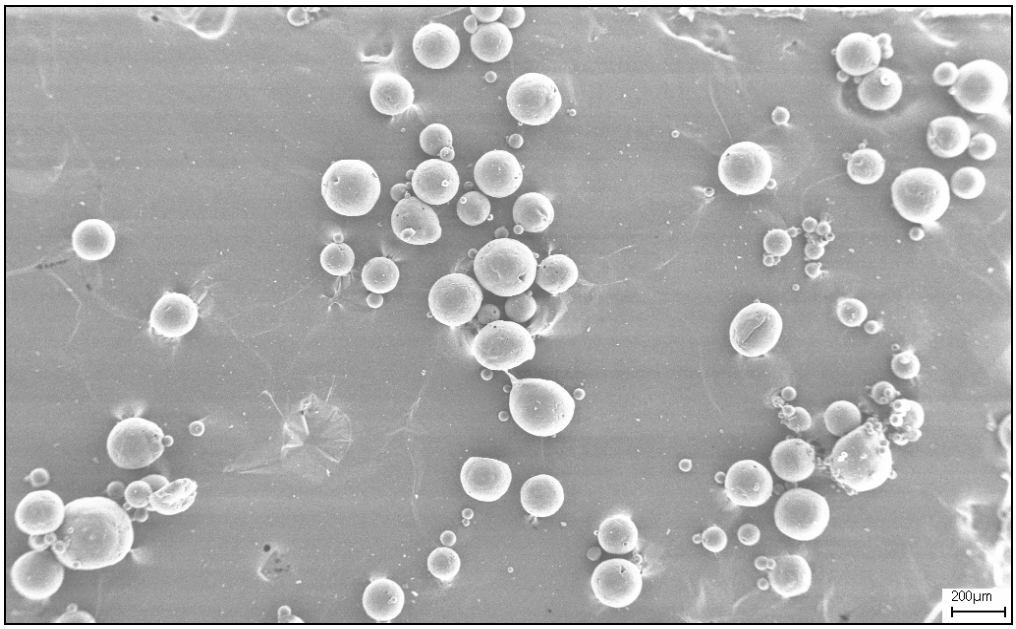

Figure 14. SEM micrographs of (a) smaller porogen and (b) larger porogen (scalebars = 200µm)

4.2 Water Phase Variables

4.2.1 Emulsion Temperature

The emulsion temperature used is known to affect specific aspects of the microparticles. Figure 15a demonstrates that with an increase in temperature from 11℃ to 35℃, the average particle size was seen to fluctuate with a size below 200µm only being achieved at room temperature. In Figure 15b, an 81% volume yield in the 50-200µm size range was achieved at the same temperature while any temperature above as well as below this, resulted in yields lower than 50%. The hemi-shell yield was found to increase to 27% at room temperature and increased slightly at 33℃.

The emulsion temperature is known to affect emulsion stability due to the density and viscosity fluctuations (Lissant K.J, 1974). These fluctuations in temperature have also been investigated by Yang et al (2000) whom also found a similar trend to that shown in Figure 15. The optimum temperature

appears to be at room temperature whereby the average microparticles size and volume yield in the desired size range are the highest. Even though the hemi-shell yield is seen to increase slightly at higher temperatures, the lower volume yield and higher standard deviation makes reproducibility at higher temperatures difficult. As a result, room temperature was found to be the optimum.

(a)

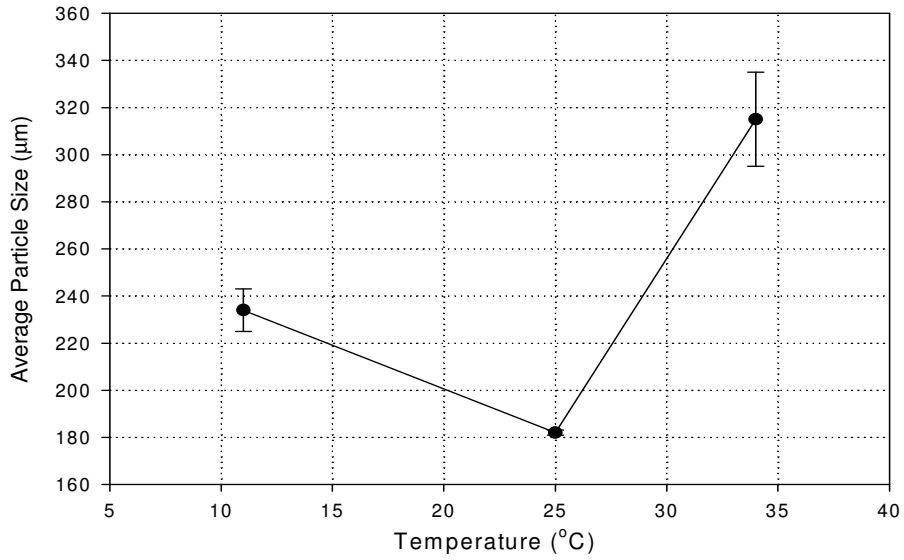

(b)

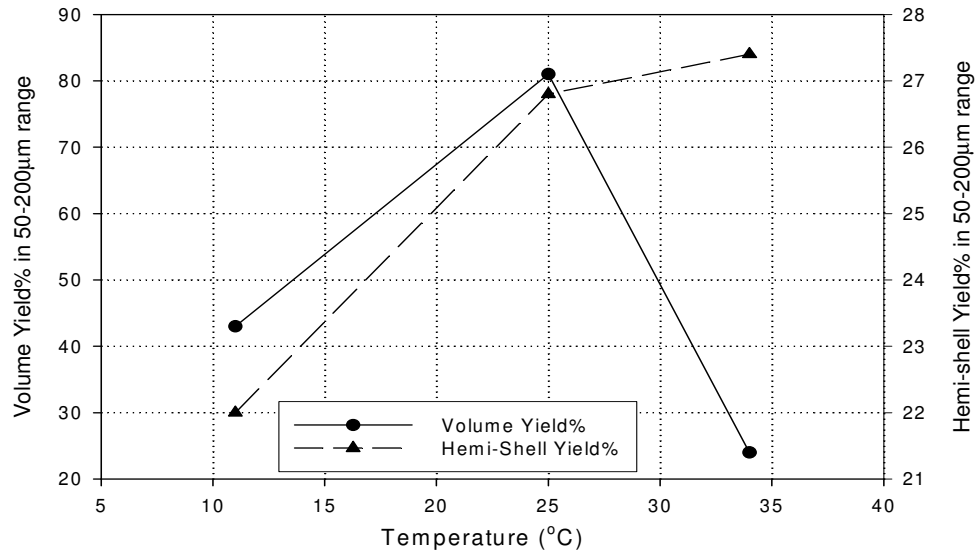

Figure 15. Effect of water phase temperature on the (a) average microparticles size and (b) volume yield% in the 50-200µm size range

4.2.2 Surfactant Molecular Weight & Solvent Evaporation

Different solvent evaporation processes such as vacuum and fume-hood solvent evaporation can result in varying particle sizes as well as porosity. It is also known that the surfactant molecular weight can play a role in the size obtained during emulsification (Murakami et al, 1997). As such, high and low molecular weight polyvinylalcohol (PVA) grades (Table 5) were investigated under different solvent evaporation conditions but with a fixed PVA concentration (1% w/v) and similar degrees of hydrolysation of 85-89%.

As shown in Figure 16a and b, high molecular weight (Mw) PVA under fume-hood results in a larger average particle size than the lower Mw PVA while the inverse happens under vacuum solvent evaporation conditions of 750mbar. As usual, an inverse relationship existed between the volume particle yield and the average particle size obtained. It is difficult to postulate as to reason for such a result but in terms of scale-up and process control simplicity, the low surfactant Mw and fumehood conditions were selected as optimum for further use. Qualitative morphology observation of the microparticles from this sample also showed a similar yield of hemi-shells in comparison to the others (Data not shown).

Table 5. Properties of polyvinylalcohol grades

Grade	Viscosity (cps)	% Hydrolysis
Polinol P17	21-24	85.5-88.5
Sigma	3.5-4.5	87-89

(a)

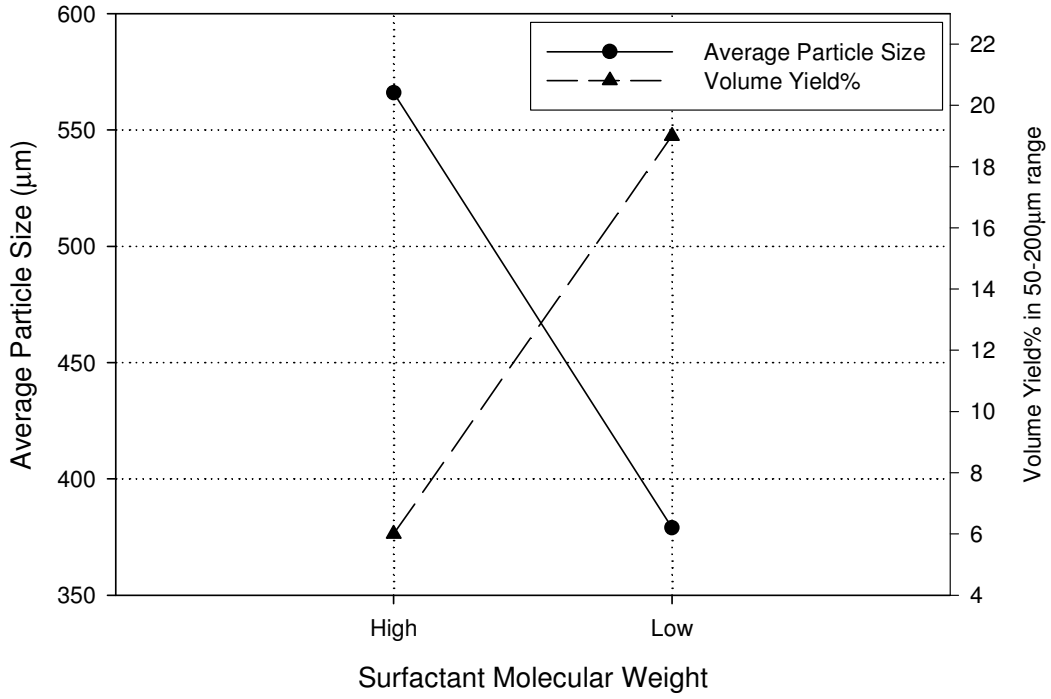

(b)

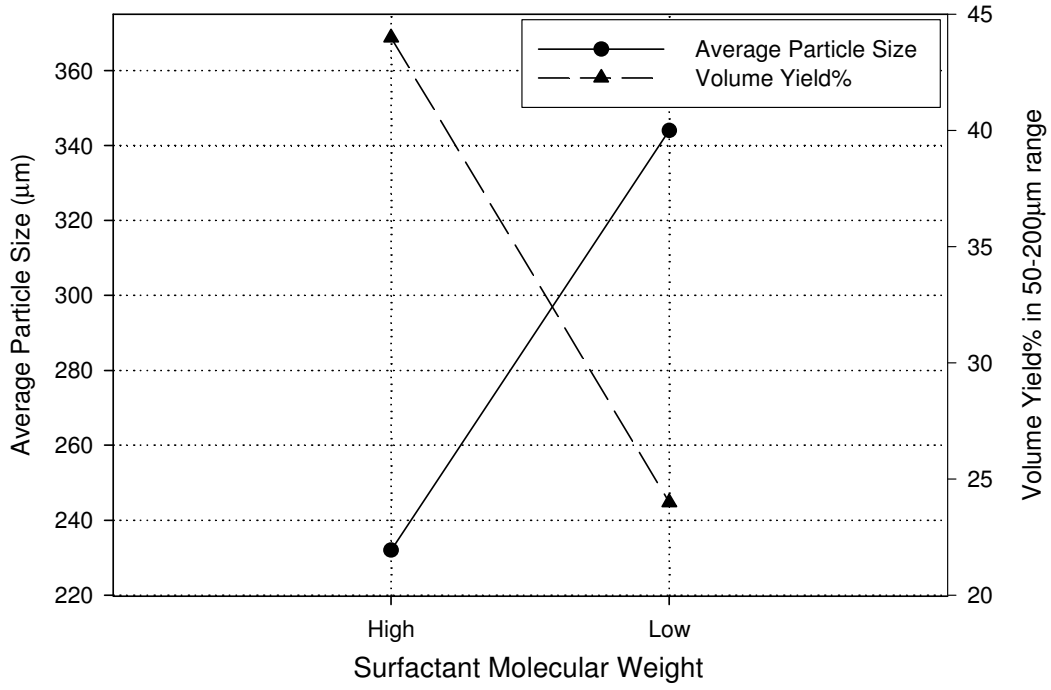

Figure 16. Effect of polyvinylalcohol molecular weight on the average particle size and volume yield% in the 50-200µm range for (a) Fume-hood and (b) vacuum solvent evaporation

4.3 Emulsion Formation Variables

4.3.1 Homogeniser Speed

Homogenisation is known to be useful in controlling the microparticles particle size distribution (Feng et al., 2005). Due to the previous interaction of microparticles size with porogen shear while homogenising, two different porogen size fractions were investigated while homogenising at various homogenisation speeds.

Figure 17 demonstrates that as homogenisation speed was increased from 300rpm to 600rpm, the average microparticles size, as expected, decreased for both samples irrespective of the porogen size fraction used. There was however a significant decrease in the average particle size when homogenisation speed was increased for the 100-150µm porogen size fraction.

The hemi-shell yield was seen to fluctuate with the homogenisation speed but the maximum yield of 32% was found at the lowest homogenisation speed of 300rpm (Figure 18) for the 25-38µm porogen. This can be attributed to porogen shear effects coupled with increased porogen loss from the polymer-oil phase resulting in a fluctuating hemi-shell yield.

Unlike the smaller porogen, the hemi-shell yield for the larger porogen was at a maximum of 21% at 400rpm. However, this was still a lower hemi-shell yield in comparison to the smaller porogen at a lower homogenisation speed of 300rpm. The particle volume yield behaved inversely to the average particle size again, with higher volume yields being obtained as speed was increased. The standard speed of 300rpm was still found to be optimum as it provided the highest hemi-shell yield when the smaller porogen size fraction was used and at a lower homogenisation speed.

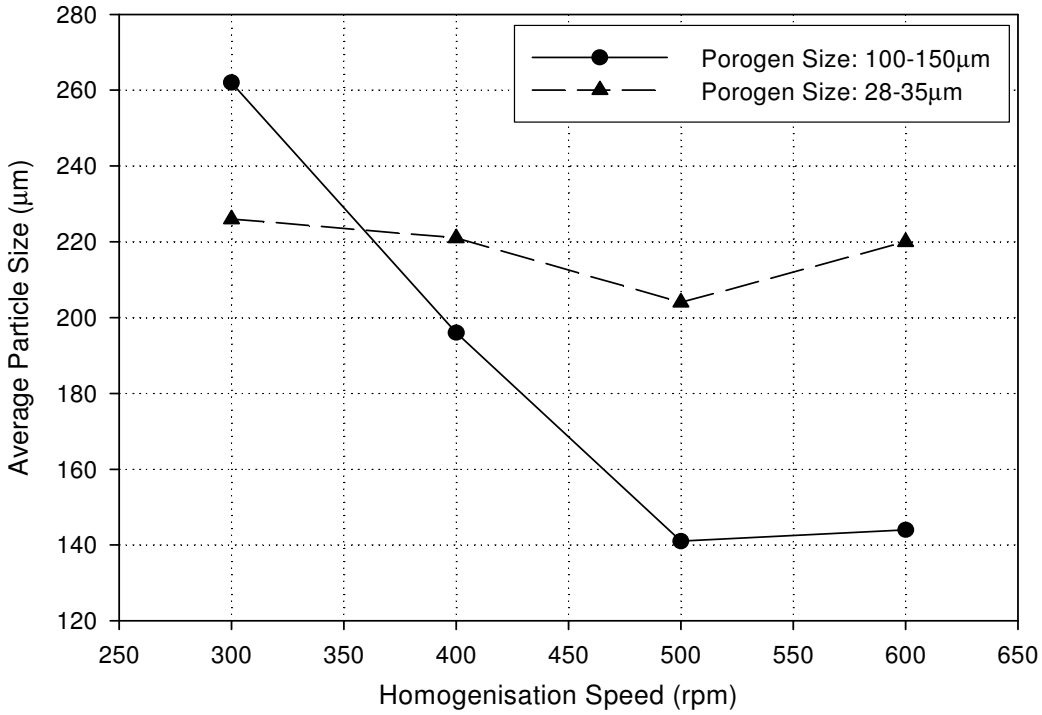

Figure 17. Effect of homogenisation speed on average particle size

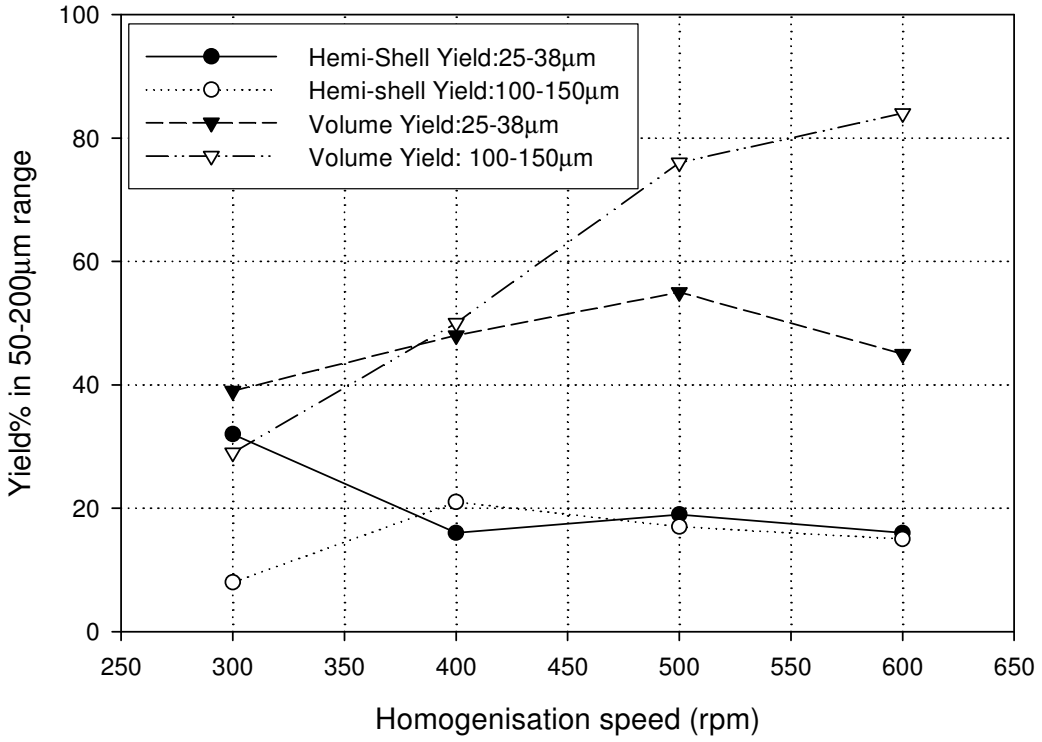

Figure 18. Effect of homogenisation speed on the hemi-shell and volume yield% in the 50-200µm range

4.3.2 Homogenisation Type

The type of mixing device employed is known to affect the particle size as well as morphology obtained during emulsification (Rosca et al., 2004). Figure 19 shows the effect of magnetic stirring only compared to homogenisation at 300rpm for 2minutes followed by magnetic stirring. Even though homogenisation did result in a slightly lower volume yield yet higher reproducibility than magnetic stirring, the qualitatively higher hemi-shell yield that was observed, made it the preferred process.

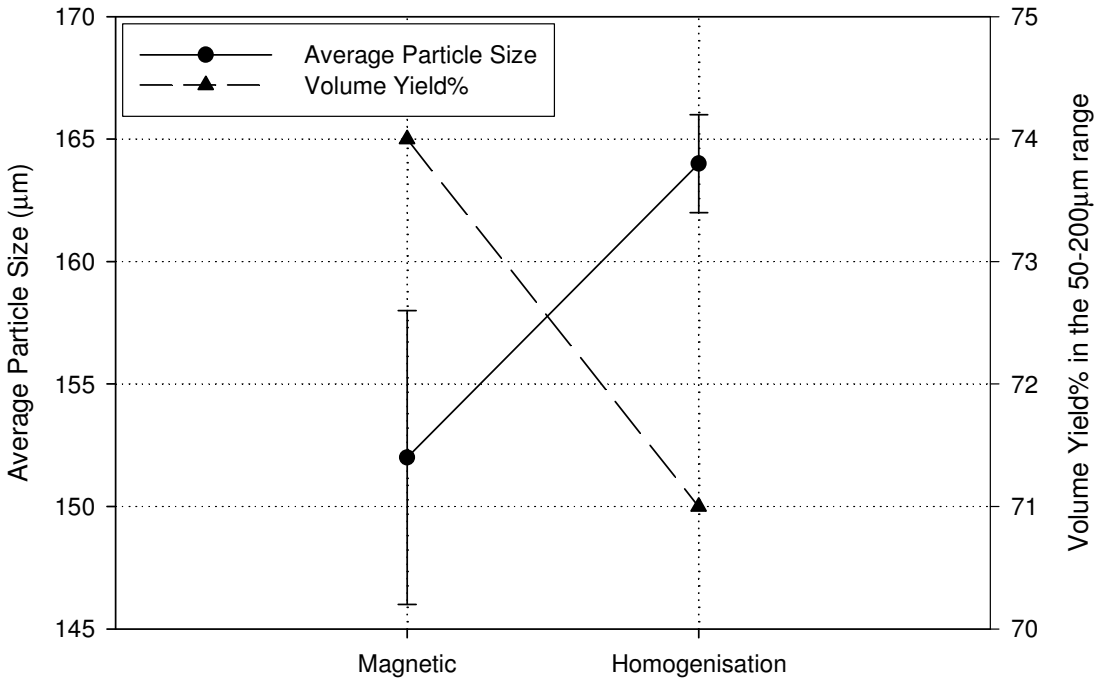

Figure 19. Effect of magnetic stirring compared to homogenization on the average particle size and volume yield% in the 50-200µm range

4.4 Microparticles Characterisation

4.4.1 Reproducibility Studies

After investigation of all the above variables, the method which yielded the most hemi-shells in the desired 50-200µm range was selected for further reproducibility studies. This was important as the need for a reproducible process was required if future scale-up was to be feasible. The final process variables that were selected at each step are displayed in Figure 20.

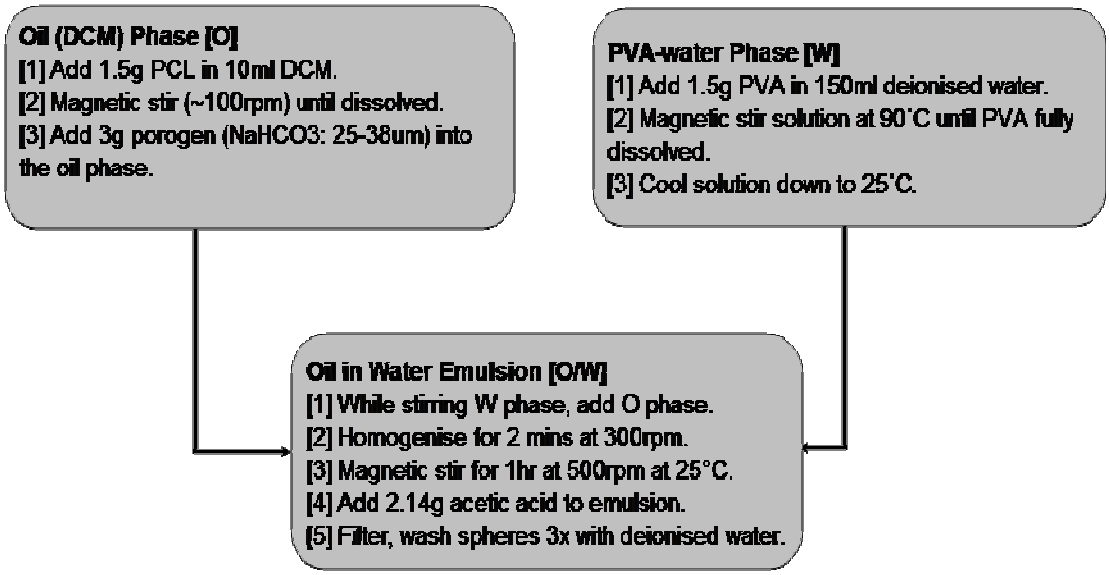

Figure 20. Composition and method used in hemi-shells fabrication

The parameters used to evaluate reproducibility were the average particles size (Figure 21), mass yields (Figure 22) and the hemi-shell yields in the 50-200µm range (Figure 22). A comparison was also made between the average microparticles sizes and that of the hemi-shell sizes as determined from optical micrographs (Figure 23) which can be seen to be similar to the average particles size.

The mass yield recovered after emulsification was found to be on average about 80%. A further 25-30% mass loss occurs when sieving the microparticles into the desired 50-200µm size range. Hence, the average

mass yield of particles in the desired size range containing hemi-shells was about 50%. The 50% mass loss can be attributed to the typical process related mass losses such as polymer that adheres to the homogeniser and magnetic stirrer bar as well as sieving mass losses. From optical micrographs analysis, the number-averaged hemi-shell yield was found to be on average 40%. Due to difficulty of hemi-shells separation, an adequate separation method is still being investigated.

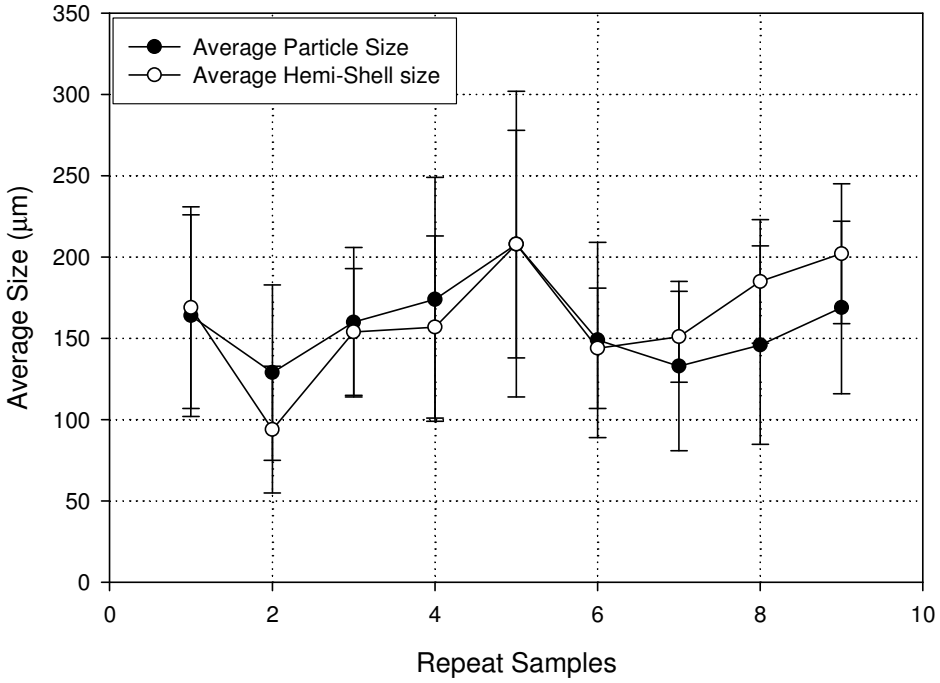

Figure 21. Reproducibility samples analysis with average particle and hemi-shell sizes

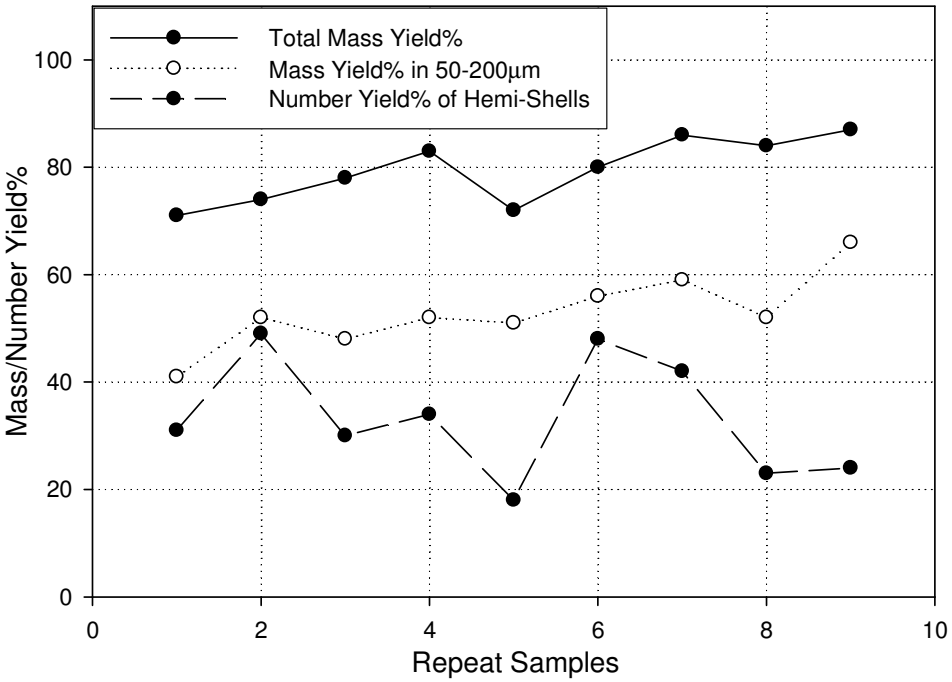

Figure 22. Reproducibility samples mass yields

A number of optical and SEM micrographs were taken of the repeated standards and these were compared in order to investigate sample representavity. Figure 23 shows two such micrographs from repeated micrograph sample analysis. They were found to be qualitatively similar in terms of morphology and microparticle sizes. As shown, the visualisation of hollow particles and internal particle porosity is not possible via SEM unlike optical microscopy. Also due to the smaller sample size used in SEM, far greater hemi-shells could be seen in optical micrographs hence these were used in hemi-shells yield analysis.

(a)

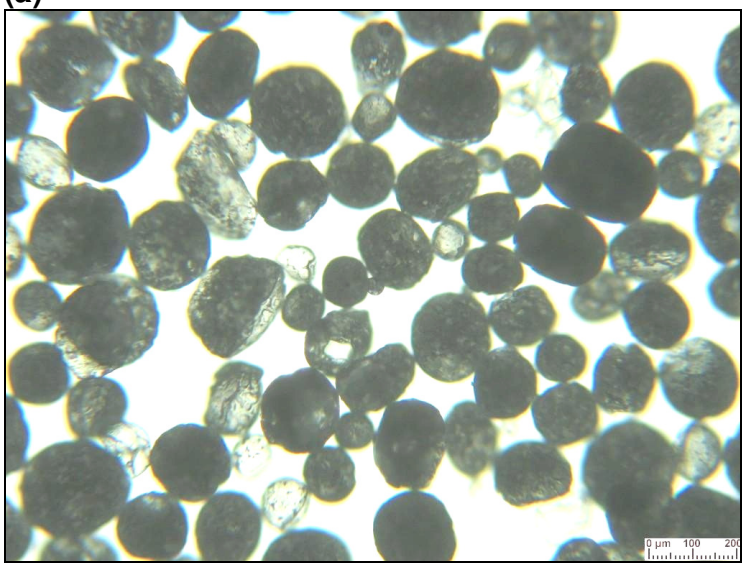

(b)

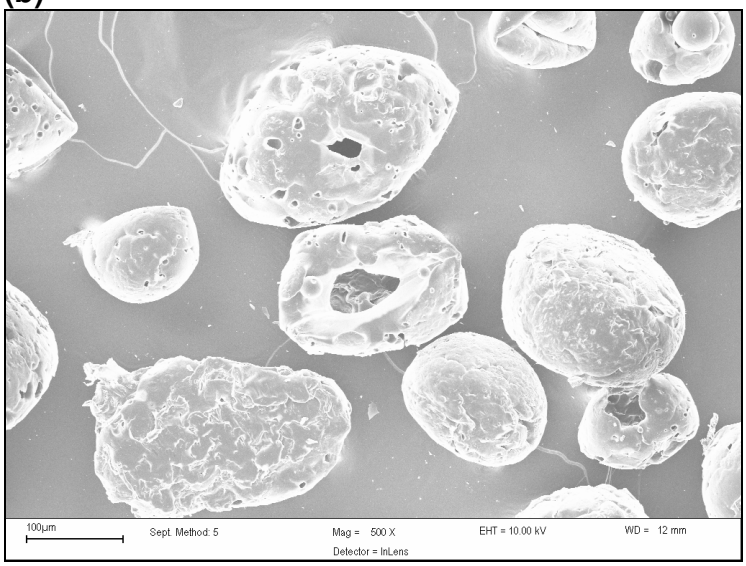

Figure 23. Comparison of an (a) optical to a (b) SEM micrograph

4.4.2 Energy-Dispersive X-Ray Spectroscopy (EDX)

Scanning electron microscopy (SEM) with an EDX attachment was applied to detect the chemical elements present on the surface of the microparticles. A number of spectra were obtained and one such spectrum was shown in Figure 24. No sodium from the sodium bicarbonate porogen was detected on the microparticle's surface. This possibly indicates that the microparticles washing process is fairly efficient at removal of any unwanted surface ions.

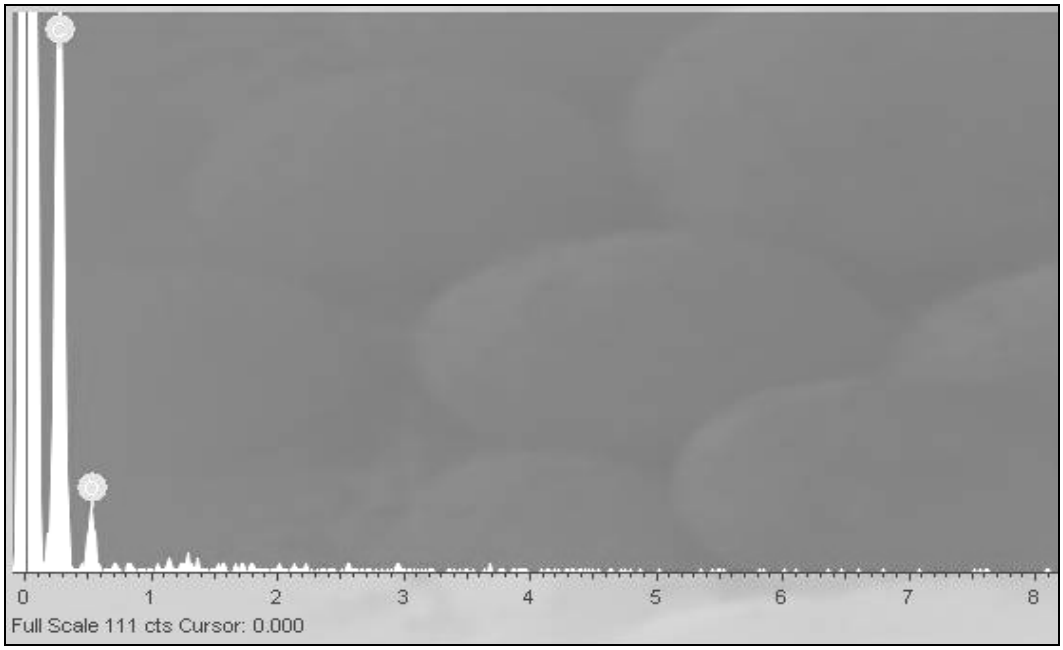

Figure 24. EDX spectra of the microparticle's surface

4.4.3 Confocal Laser Scanning Microscopy (CLSM)

CLSM was used to investigate the porosity and surface roughness of the microparticles. This was achieved by using fluorescent labelling using Nile Red (excitation = 550nm, emission = 650nm). Since Nile Red is soluble in DCM, it was dissolved in the oil-polymer phase at a concentration of 1mg/ml.

This allowed for the observation of the internal porosity by use of z-stack images without requiring physical slicing through the microparticles. Such a z-stack and optical micrograph of the same microparticle is shown in Figure 25. The visual limitation in imaging of these microparticles cross section is due to the large microparticles size and the lack of polymer transparency in order for the laser to pass through.

(a)

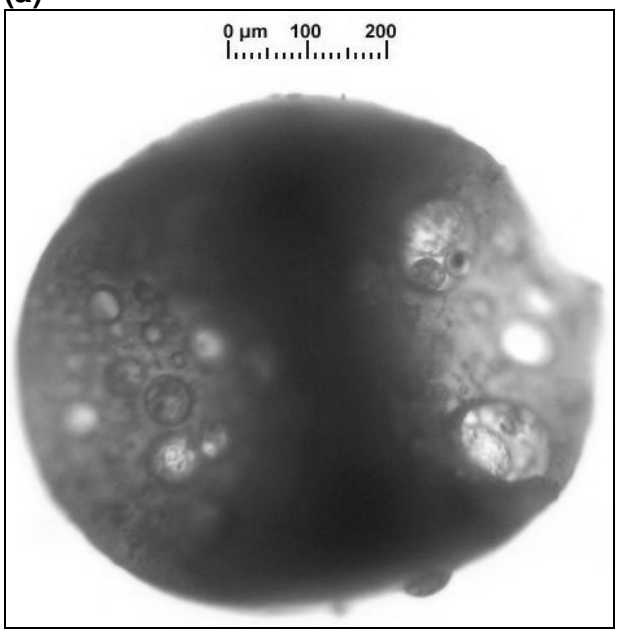

(b)

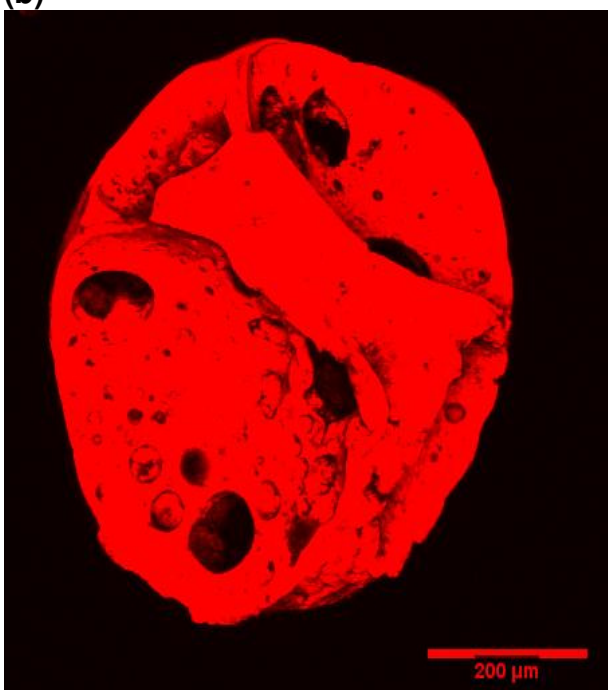

Figure 25. (a) Optical micrograph and (b) CLSM 3D projection of a porous microparticle (scalebars = 200µm)

Due to the above-mentioned problem of limited polymer transparency using the fluorescent label, the light reflectance mode was applied to obtain the microparticles surface topography (Figure 26). The surface was seen to have submicron roughness (this was seen from reflectance measurements but

these results are not included) as well as having high surface porosity. Pores of up to 20µm in diameter were seen from the pixel intensity change of the microparticle's surface (Figure 27). This pore size is adequate for cell ingrowth and attachment as cells are typically smaller than 20µm.

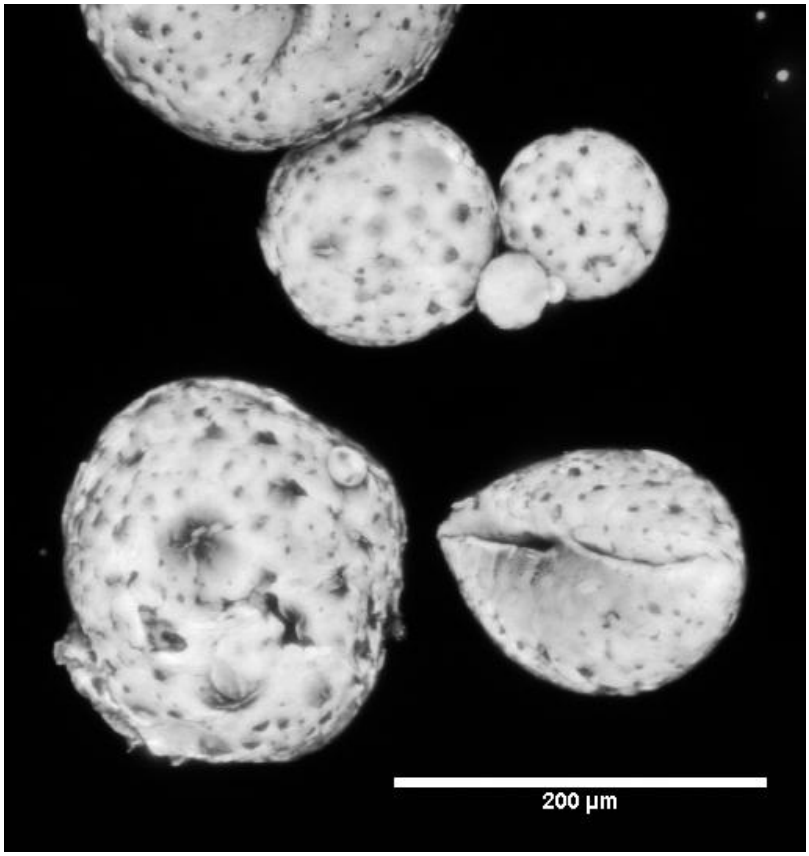

Figure 26. Light reflectance mode on microparticles (scalebar = 200µm)

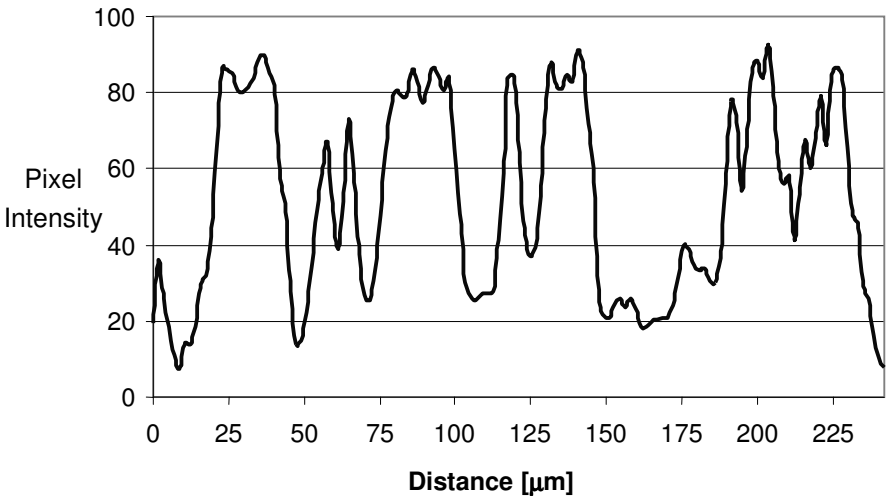

Figure 27. Surface profile using pixel intensity change over the microparticle surface

Depth colour profiling was also undertaken to illustrate the visualisation problems experienced with a microparticle in the required size range of 50-200µm (Figure 28). It was seen that due to the lack of polymer transparency, only 100µm into the particle could be seen. This was also confirmed by the 3D y-axis projection. Also seen was a porosity increase from the particle surface to the interior as shown by the 35µm z-stack image from the interior of the particle.

This porosity increase from the interior possibly indicates that gas evolution begins from within the polymer encapsulated porogen and gradually dissipates outwards. As the solvent evaporates and the polymer hardens, the gas spaces get entrapped resulting in a larger internal porosity (Rosca et al., 2004).

When these internal gas spaces coalesce during solvent evaporation, a hemi-shell or hollow microparticle can result. It was also observed that the internal porosity seems to be interconnected which is preferred for promoting cellular ingrowth (Kim et al., 2006). An approximate porosity calculation obtained using ImageJ indicated a 30-40% internal porosity from a SEM micrograph of the cross-section of a microparticle (Figure 29) and was also qualitatively observed from confocal z-stack images.

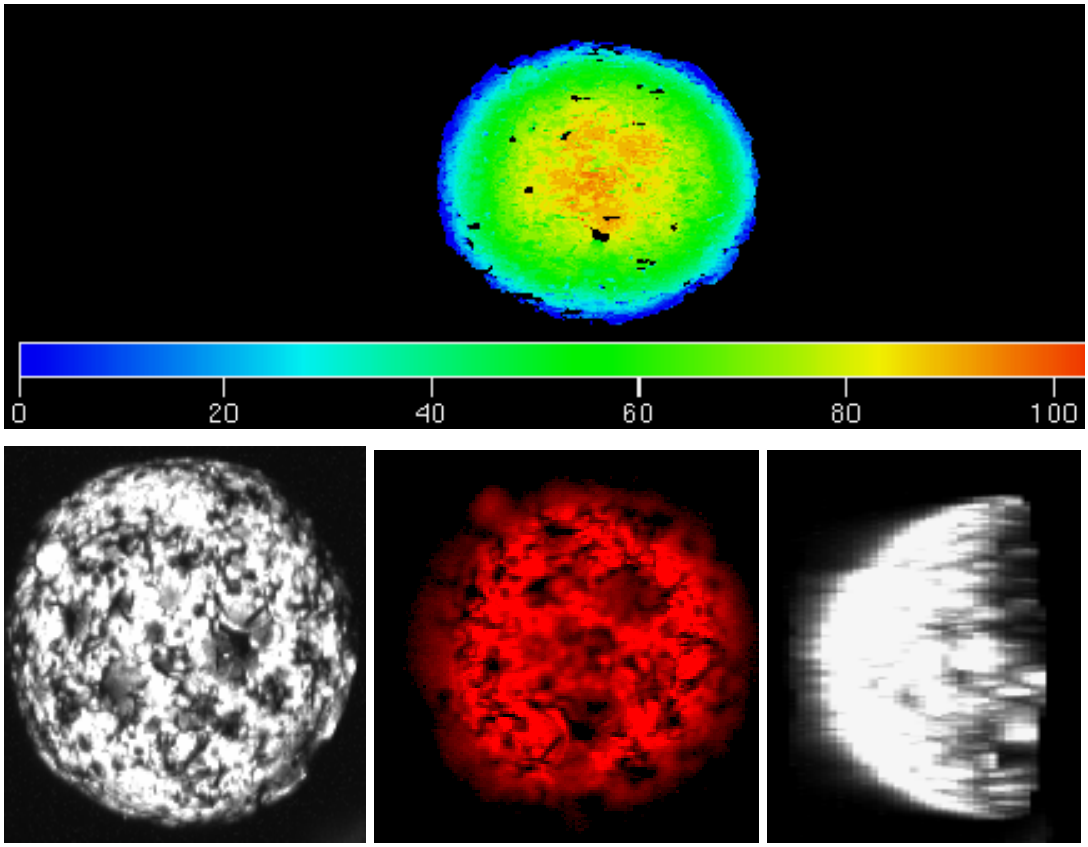

Figure 28. Top: Depth colour projection, bottom left: 3D z-projection of a 200µm sphere, middle: z-stack as seen 35µm from top & right: y-axis 3D projection

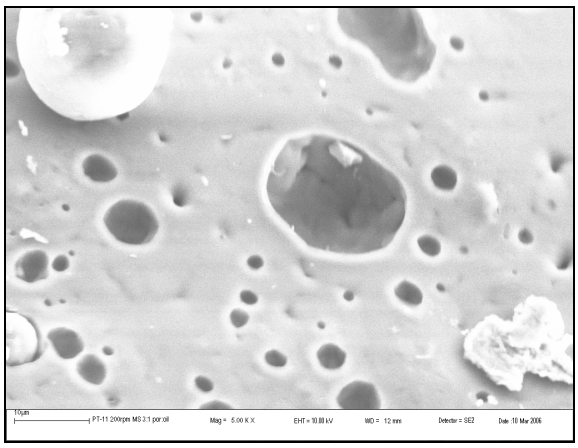

Figure 29. Cross-section through a microparticle (scalebar = 10µm)

4.4.4 Drop Shape Analysis (DSA)

Interfacial porogen behaviour was investigated using a drop shape analyser. This simulation of porogen behaviour was not as complex as the actual emulsification process. The standardised emulsion composition of porogen-polymer-DCM oil phase was pushed through a 21 gauge needle into a PVA-water phase (1% w/v) and imaged using Kruss DSA software.

It was observed that the 25-38µm porogen immediately went to the oil-water interface due to its high density (Figure 30). Some porogen was seen to fall into the PVA-water phase. This porogen motility to the interface provides some insight as to why the smaller porogen was better than the larger porogen as well as why a higher oil phase viscosity resulted in more hemi-shells as was seen previously.

A possible pathway to the different particle morphologies was concluded from these observations (Figure 31) which was found to be similar to particle morphologies as seen in SEM & optical micrographs. During emulsification, a porogen encapsulated polymer microparticle, could follow many different pathways to arrive at the final particle morphology. Depending on the porogen location and the resulting gas formation and coalescence within the polymeric matrix, microporous or hollow or hem-shell microparticles could be formed. A further experiment, as described in the following section, was used to study the formation of the hemi-shells in more depth.

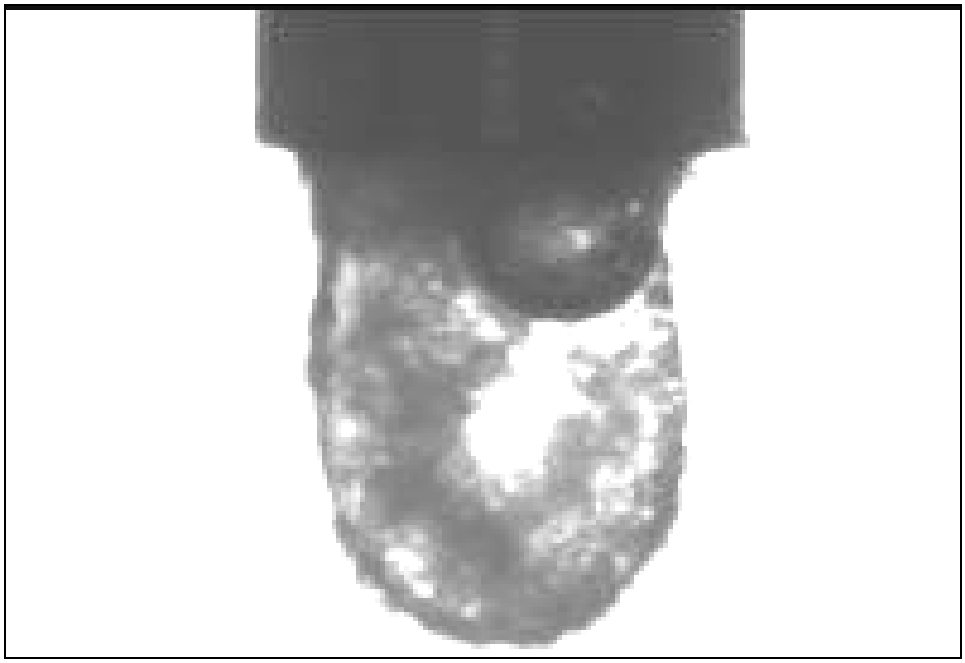

Figure 30. Interfacial behaviour of DCM droplet in PVA-water phase

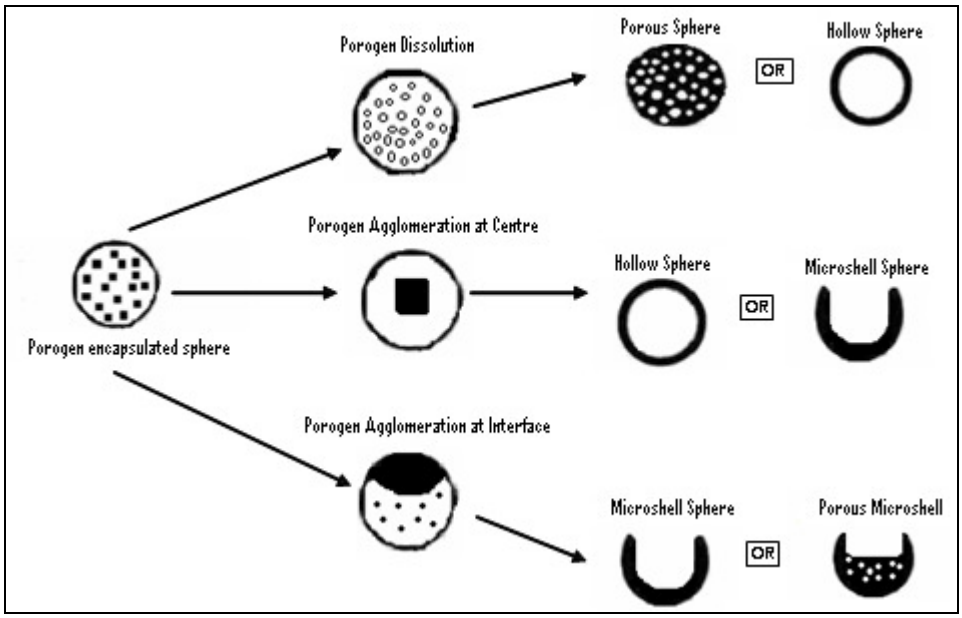

Figure 31. Schematic of various particle morphology development routes

4.4.4 Optical Tracking

Figure 32 shows the morphological changes observed in the stages of hemi-shell development with time as observed using optical microscopy while still wet. After 10 minutes of solvent-evaporation (Figure 32a), the porogen

dissolved forming carbon dioxide (CO_2) gas bubbles which were encapsulated within the solidifying polymeric matrix

These gas bubbles gradually coalesced forming larger bubbles as seen at 20 and 30 minutes (Figure 32b, c). It is hypothesized that these gas bubbles once fully coalesced (Figure 33), eventually burst thus creating an internal cavity with an externally microporous shell as shown in the SEM micrograph (Figure 32d).

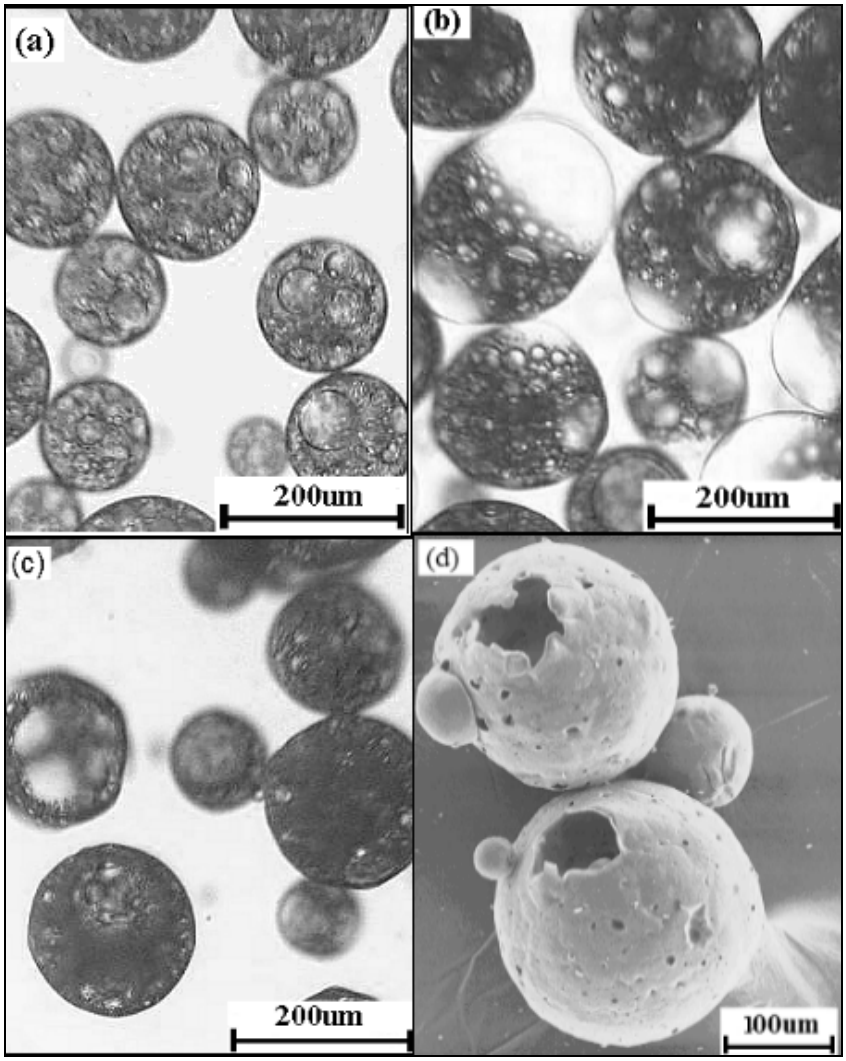

Figure 32. Optical micrographs of the hemi-shell morphological development with time: (a) 10mins, (b) 20mins, (c) 30mins and (d) SEM micrograph of the final morphology after solvent evaporation was completed

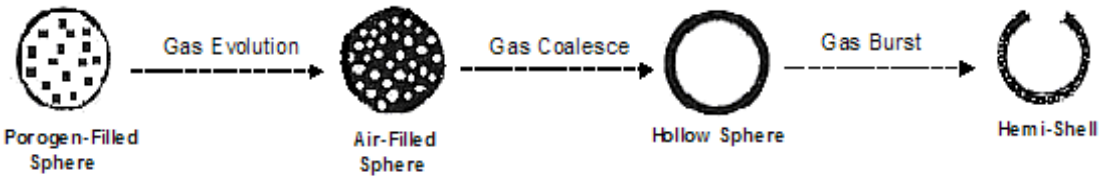

Figure 33. Schematic of hemi-shell formation

Acid addition also increased the gas formation thus creating more microporosity. Coalescence of smaller bubbles to form larger bubbles can be attributed to the change in Laplace pressure (Tadros et al., 2004):

$$P_{inside} - P_{outside} = \frac{2\sigma}{r} \quad \text{.....(3)}$$

where $P_{inside,\ outside}$ is the internal and external pressure, respectively on the bubble, r is the bubble radius and σ is the surface tension. Gas evolution was also monitored by Kim et al (2006) in the formation of poly (lactic-co-glycolic acid) (PLGA) interconnected porous particles when using ammonium bicarbonate as a porogen in a water-in-oil-water (W/O/W) emulsion.

Figure 34 illustrates the change in the number-average particle size and hemi-shell yield with solvent evaporation time as calculated optical micrographs captured. The number-average particle size decreased with time from 163µm to 149µm as solvent evaporation progressed from 10 to 75minutes. A number-average particle yield of 84% was obtained in the 50-200µm range after solvent evaporation was completed. The microparticle size decrease corresponded to an increase in hemi-shell yield whereby a final yield of 41% was achieved after 75minutes.

The increase in hemi-shell yield as explained above could be due to the increase in bubble coalescence as the polymeric microparticles shrink during solvent evaporation which is analogous to the coalescence seen in W/O/W emulsions (Crotts et al., 1995 & Kim et al., 2006).

The hemi-shell formation thus can be seen to be influenced by such factors

such as the oil phase viscosity, homogeniser speed etc as described previously. Since it is important to retain as much porogen microparticles within the polymer matrix to generate enough gas to form a hemi-shell, oil phase viscosity would need to be high as possible. This was accomplished by the maximum polymer concentration of 15% w/v in the oil phase.

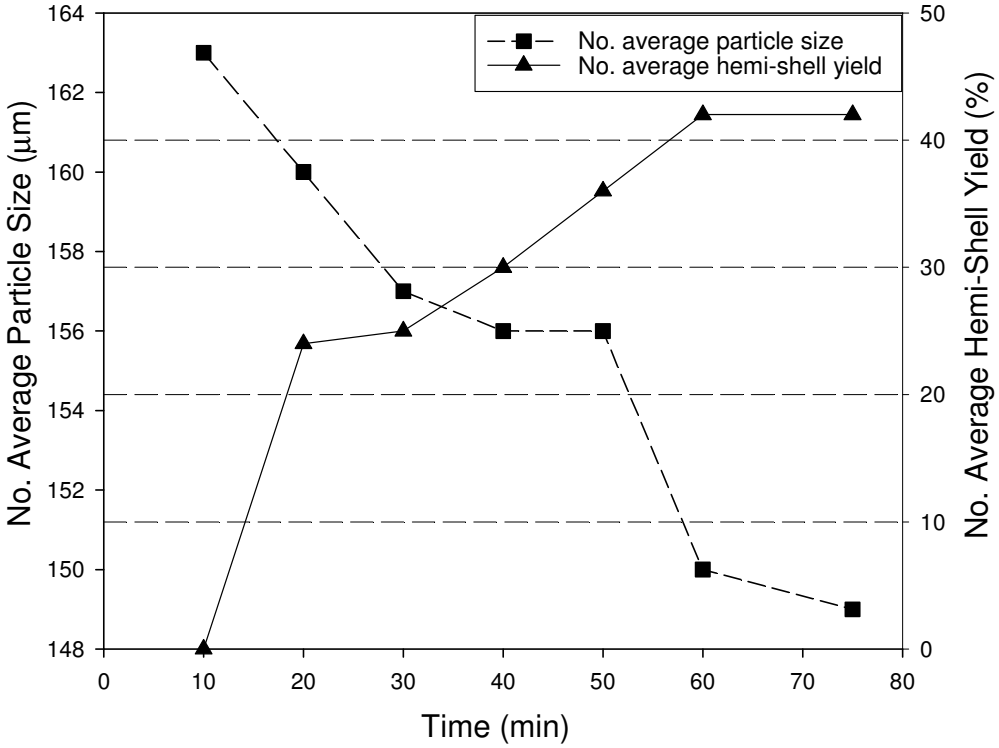

Figure 34. Plot of change in number-averaged particle size and hemi-shell yield with solvent evaporation time

4.4.5 Residual Solvent Analysis

Solvent extraction was used for the analysis of the residual DCM within the microparticles. This was done by weighing out 50mg of polymeric microspheres into a 2ml vial. Methanol (500µl) was selected as the extraction solvent as it did not dissolve the polymer, possessed a high affinity for DCM and did not co-elute with methanol. Solutions were mixed by vigorous shaking for 10minutes and left to stand for 24hours. After extraction, solutions were filtered into a 2ml vial and the solution was injection ready. Samples were conducted in triplicate.

As a control, 50mg of the polymer was weighed and spiked with 5µl of DCM. DCM was quickly absorbed by the polymer after mixing through shaking while with a closed vial. The spiked vial was left standing for 24hours and DCM was extracted as before.

The non-spiked DCM extracted sample was analysed and no peak was obtained for DCM (Figure 35). This clearly indicates that no DCM was extracted from the samples. To make sure that the absence of DCM was due to no or little residual solvent in the polymer and not because of poor methanol extraction, the sample was spiked with a known quantity of DCM, left to stand for 24hours and then extracted using the same method.

Figure 36 illustrates the chromatogram obtained and that the DCM peak was clearly visible. The other peak appearing at around 20minutes was attributed to an unknown substance coming out of the chromatographic system and it was seen in the runs including the standards from direct injection and hence was not obtained from the microparticles.

Figure 37 was the chromatogram obtained by overlaying the extracted non-spiked sample and the sample spiked with a known amount of DCM. The detection limit for DCM was found to be 0.38ppm by using stock dilutions of methanol and DCM. The residual DCM could not be detected hence it would be less than 0.38ppm which is much lower than the medically permitted level of 600pm hence acceptable for use in soft tissue augmentation applications.

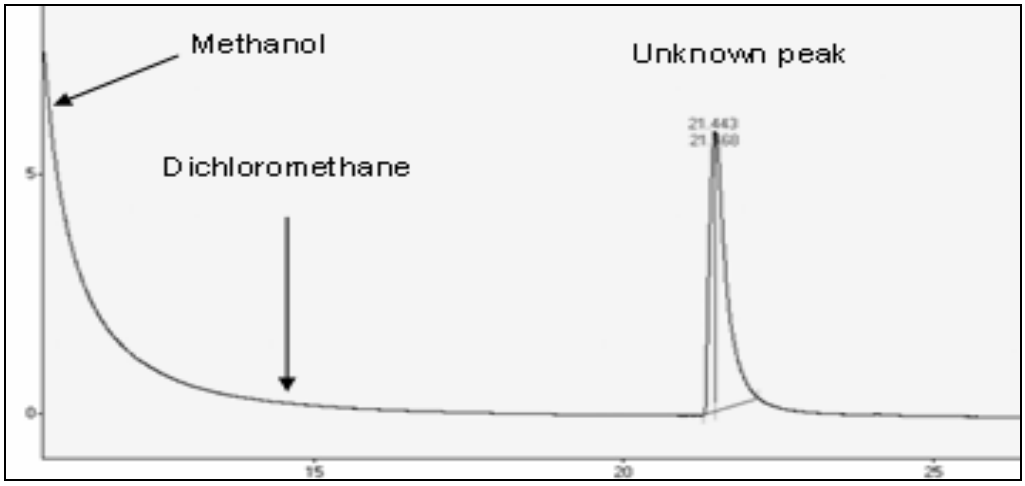

Figure 35. Chromatogram obtained after methanol extraction of microspheres

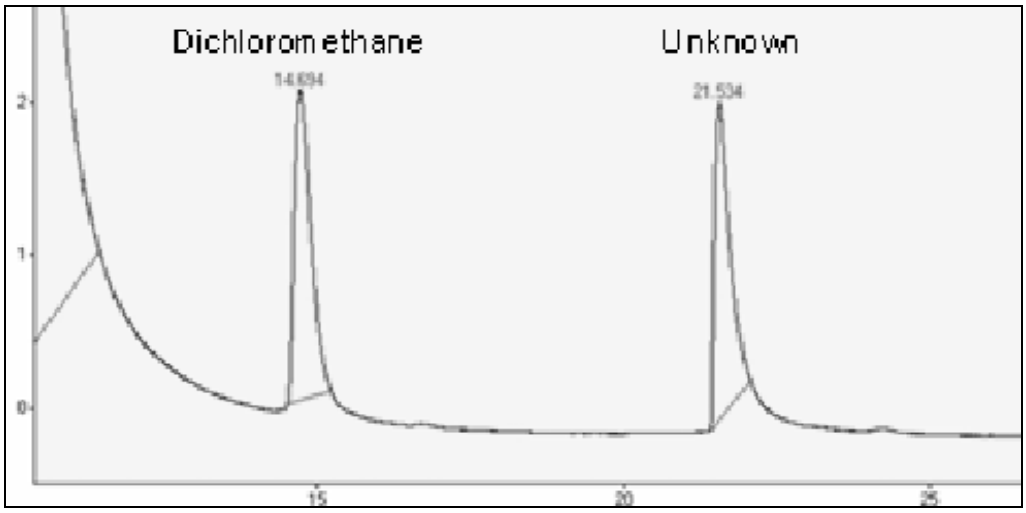

Figure 36. Chromatogram obtained after methanol extraction of microspheres, spiked with known amount of DCM

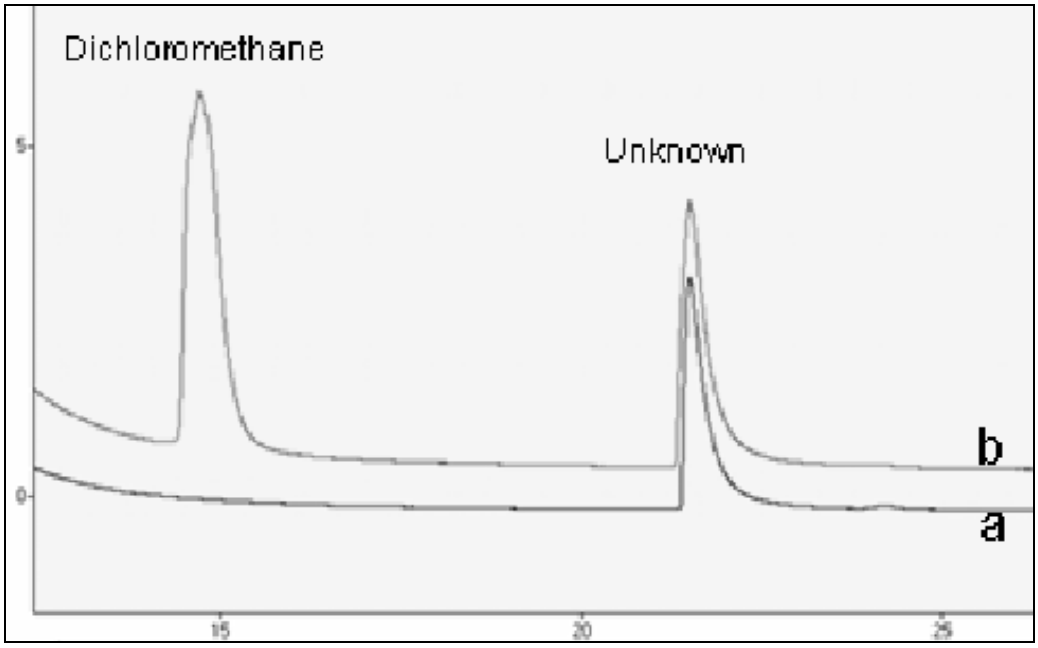

Figure 37. Chromatogram obtained after methanol extraction of (a) standard synthesis microparticles and (b) spiked with known amount of DCM

5. Conclusions and Future Work

Novel microporous polycaprolactone hemi-shells with a number-average particle yield of 84% in the 50-200µm range have been successfully produced by sodium bicarbonate addition into a modified oil-in-water emulsion with a final mass yield of hemi-shells from this process found to be about 50%. The unique morphology has potential applications in tissue engineering, and drug delivery amongst others and the current manufacturing process has been patented (Naidoo K et al., 2006).

Gas evolution from porogen dissolution leads to a highly porous microparticle at the onset, which finally develops into a hollow concavity with a microporous shell. Gas coalescence as solvent evaporates coupled with microparticle hardening lead to the desired formation of the unique morphology. Hemi-shells displayed central openings of up to 75µm in diameter with surface micropores up to 20µm in diameter.

Numerous process factors were investigated in order to elucidate the morphology mechanism of formation. Porogen loading and size, oil viscosity and homogenisation speed were deemed to play a significant role in the hemi-shell morphology formation. Porogen loss from the dichloromethane-polymer phase and dissolution into the aqueous phase resulted in a lower hemi-shell yield. Hence, reducing oil viscosity and process factors that result in greater porogen loss from the polymeric microparticle matrix lead to diminished hemi-shells.

Further studies need to be conducted in order to increase the hemi-shell yield by isolation of the desired hemi-shell morphology. Also, further proof of concept studies need to be conducted by doing *in-vitro* and *in-vivo* trials in order to investigate if mammalian cells will attach, proliferate and preferentially migrate into the hemi-shells. The potential incorporation of drugs and other biological additives into or unto the hemi-shells can also be investigated in future studies.

6. References

Aho AJ, Tirri T, Seppala J, Rich J, Strandberg N, Jaakkola T, Narhi T, Kukkonen J, Bioactive glass-polymer composite for experimental bone reconstruction, Key Engineering Materials, 192-1: 685-687, 2000.

Aracil Kessler JP, Diaz Torres JM, Martin Garcia RF, Artecoll: An experimental study, Cir Plast Ibero-Latinoamer, 23: 389, 1997.

Ashinof R, Overview: Soft Tissue Augmentation, Clinics in Plastic Surgery, 27: 4, 479-487, 2000.

Bergeret-Galley C, Latouche X, Illouz YG, The value of a new filler material in corrective and cosmetic surgery: DermaLive and DermaDeep, Aesthetic Plastic Surgery, 25:4, 249-255, 2001.

Berke GS, Blumin JH, Sebastian JL, Keller GS, Revazova ES, Vocal cord augmentation with cultured autologous fibroblasts, Bulletin Exp Bio & Med, 30:8, 790-792, 2000.

Bittner B, Morlock M, Koll H, Winter G, Kissel T, Recombinant human erythropoietin (rhEPO) loaded poly(lactide-co-glycolide) microspheres: influence of the encapsulation technique and polymer purity on microsphere characteristics, Eur J Pharm & BioPharm, 45, 295-305, 1998.

Capozza N, Patricolo M, Lais A, Matarazzo E, Caione P, Endoscopic treatment of vesico-ureteral reflux: Twelve years' experience, Uroligca Int, 67:3, 228-231, 2001.

Cheng JT, Perkins SW, Hamilton MM, Collagen and injectable fillers, Otolaryngolic Clinics of North America, 35:1, 73, 2002.

Chertin B, Colhoun E, Velayudham M, Puri P, Endoscopic treatment of vesicoureteral reflux: 11 to 17 years of follow-up, J. Urology, 167:3, 1443-

1445, 2002.

Courey MS, Homologous collagen substances for vocal fold augmentation, Laryngoscope, 111:5, 747-758, 2001.

Dmochowski RR, Appell RA, Injectable agents in the treatment of stress urinary incontinence in women: where are we now?, Urology, 56 (Suppl A):32-40, 2000.

Edwards DA, Hanes J, Langer R, Large porous particles for pulmonary drug delivery, Science, 276, 1868–1871, 1997.

Einmahl S, Capancioni S, Schwach-Abdellaoui K, Moeller M, Behar-Cohen F, Gurny R, Therapeutic applications of viscous and injectable poly(ortho esters), Advanced Drug Delivery Reviews, 53:1, 45-73. 2001.

Feng SS, Li QT, Ruan G, Effects of material hydrophobicity on physical properties of polymeric microspheres formed by double emulsion process, J Controlled Release, 84:151-160, 2005.

Fox C, Rationale for the selection of emulsifying agents, 101, 25-44, 1986.

Furness PD, Kolligian ME, Lang SJ, Kaplan WE, Kropp BP, Cheng EY, Injectable small intestinal submucosa: Preliminary evaluation for use in endoscopic urological surgery, J. Urology, 164:5, 1680-1684, 2000.

Hakkinen A, Hirvonen J, Karjalainen M, Koistinen P, Peltonen L, The effect of cosolvents on the formulation of nanoparticles from low molecular weight polylactide, AAPS PharmSciTech, 3(4): 32, 2002.

Haverkorn RM, Gomelsky A, Bulking agents for stress urinary incontinence: Are they still indicated?, Current Bladder Dysfunction Reports, 3:26-31, 2008.

Hench LL, Erthridge EC, Biomaterials-An interfacial approach, Noordergraaf,

Vol 4A, New York, Academic Press, 1982.

Hong Y, Gao C, Shi Y, Shen J, Preparation of porous polylactide microspheres by emulsion-solvent evaporation based on solution induced phase separation, Polym. Adv. Technol, 16, 622–627, 2005.

Hong Z, Bo L, Guangsu H, Sound absorption behaviour of multiporous hollow polymer microspheres, Material Letters, 60, 3451–3456, 2001.

Hutmacher DW, Scaffold design and fabrication technologies for engineering tissues-state of the art and future perspectives, J Biomaterials Science-Polymer, 12:107-124, 2001.

Jeyanthi R, Thanoo BC, Metha RC, Deluca PP, Effect of processing parameters on the properties of peptide-containing PLGA microspheres, J. Control. Release, 38, 235–244, 1996.

Kamm MA, Faecal incontinence: common and treatable, Medical J. Australia, 176:2, 47-48, 2002.

Kim TK, Yoon JJ, Lee DS, Park TG, Gas foamed open porous biodegradable polymeric microspheres, Biomaterials, 27:152–159, 2006.

Klaus L, Biocompatibility of microparticles into soft tissue fillers, Seminars in Cutaneous Medicine and Surgery, 23: 214-217, 2004.

Klein AW, Skin filling-Collagen and other injectables of the skin, Dermatologic Clinics, 19:3, 491, 2001.

Larsson S, Bauer TW, Use of injectable calcium phosphate cement for fracture fixation: A review, Clinical Orthopaedics and related research, 395: 23-32, 2002.

Lissant KJ, Emulsions and emulsion technology, Part 1, 6, 1974.

Lissant KJ, Emulsions and emulsion technology, Part 2, 6, 1974.

Lissant KJ, Emulsions and emulsion technology, Part 3, 6, 1984.

Lofthouse SA, Kajihara M, Nagahara S, Nash A, Barcham GJ, Sedgmen B, Brandon MR, Sano A, Injectable silicone implants as vaccine delivery vehicles, Vaccine, 20:13-14, 1725-1732, 2002.

Lowe NJ, Maxwell CA, Lowe P, Duick MG, Shah K, Hyaluronic acid skin fillers: Adverse reactions and skin testing, J American Academy Dermatology, 45:6, 930-933, 2001.

Ma Z, Gao C, Gong Y, Shen J, Paraffin spheres as porogen to fabricate poly(L-lactic acid) scaffolds with improved cytocompatibility for cartilage tissue engineering, J Biomed Mater Res, 67B, 610-617, 2003.

Mason RJ, Hughes M, Lehman GA, Chiao G, Deviere J, Silverman DE, DeMeester TR, Peters JH, Endoscopic augmentation of the cardia with a biocompatible injectable polymer (Enteryx) in a porcine model, Surgical & Other International Techniques, 16:3, 386-391, 2002.

Mhlanga SD, Thesis on quantitative analysis for the removal of natural organic matter and degradation by-products from water using cyclodextrin nanoporous polymers, University of Johannesburg, 2004.

Mi FL, Tan YC, Liang HF, Sung HW, In vivo biocompatibility and degradability of a novel injectable-chitosan-based implant, Biomaterials, 23:1,181-191, 2002.

Murakami H, Kawashima Y, Niwa T, Hino T, Takeuchi H, Kobayashi M, Influence of the degrees of hydrolyzation and polymerization of poly(vinylalcohol) on the preparation and properties of poly(DL-lactide-co-glycolide) nanoparticle, Int J. Pharmaceutics, 149: 43-49, 1997.

Mukherjee K, Constantine G, Urinary stress incontinence in obese women: tension-free vaginal tape is the answer, Bju Int, 88:9, 881-883, 2001.

Naidoo K, Moolman S, Merwe v.d S, Bulking of soft tissue, PCT Patent: WO 2007/113762 A2, 2006.

Naoum C, Dasiou-Plakida D, Dermal filler materials and botulin toxin, Int J. Dermatology, 40:10, 609-621, 2001.

Noh I, Choi Y.J, Media tissue regeneration of the hybrid expanded polytetrafluoroethylene vascular graft via gelatin coating, Current Applied Physics, 5: 463-467, 2005.

Pannek J, Brands FH, Senge T, Particle migration after transurethral injection of carbon coated beads for stress urinary incontinence, J. Urology, 166:4, 1350-1353, 2001.

Paolino D, Ventura A, Nistico S, Puglisi G, Fresta M, Lecithin microemulsions for the topical administration of ketoprofen, Int. J. Pharmaceuticals, 21-31, 2002.

Reiss JG, Oxygen carriers ("Blood Substitutes"), Chemistry and some Physiology 101, Chem Rev, 2797-2978, 2001.

Rosano HL, Clausse M, Microemulsion Systems, Surfactant & science series, 24, 1987.

Rosca ID, Watari F, Uo M, Microparticle formation and its mechanism in single and double emulsion solvent evaporation, J Controlled Release, 99: 271-280, 2004.

Sah H, Bahl Y, Dynamic changes in size distribution of emulsion droplets during ethyl acetate-based microencapsulation process, AAPS PharmSciTech, 1:1, 2000.

Senuma Y, Franceschin S, Hilborn JG, Tissieres P, Bisson I, Frey P, Bioresorbable microspheres by spinning disk atomisation as injectable cell carrier: from preparation to in vitro evaluation, Biomaterials, 21, 1135–1144, 2000.

Simmonent JT, Sonnevill O, Lagnet S, US Patent No: 6.461.625, 2000.

Smith CP, Chancellor MB, Genitourinary tract patent update, Expert Opinion on Therapeutic Patients, 11:1, 17-31, 2001.

Tadros T, Izquiredo P, Esquena J, Solans C, Formation and stability of nano-emulsions, Advances in Colloid and Interface Science, 108-109: 303-318, 2004.

Wall SJ, Adamson PA, Augmentation, enhancement, and implantation procedures for the lips, Otolaryngologic Clinics of North America, 35:1, 87, 2002.

7. Appendix

7.1 Published Peer-Reviewed Paper

An emulsion preparation for novel microporous polymeric hemi-shells [Journal of Material Letters, 62 (2008), 252-254]

Abstract

A modified oil-in-water (O/W) emulsion process was developed to produce novel microporous hemi-spherical polycaprolactone (PCL) microparticles called “hemi-shells”. By addition of a porogen such as sodium bicarbonate ($NaHCO_3$) into the PCL-dichloromethane (DCM) oil phase and emulsification in an acidic polyvinyl alcohol (PVA) aqueous phase, microporous hemi-shells formed as solvent evaporated. CO_2 gas evolution from the porogen created particles with an externally microporous shell and a large internal cavity. The hemi-shells were characterized by SEM and optical microscopy. The number-average particle yield in the 50-200μm range was 84%. The number-average hemi-shell yield in the same size range was 41%. These novel microparticles have potential applications in tissue engineering and drug delivery.

Keywords: Emulsion; Polymers; Hemi-spherical; Microparticles; Porogen

1. Introduction

Microporous polymeric microspheres have been fabricated by many methods for a wide range of applications. Typical manufacturing methods include modified emulsion-solvent evaporation systems [1,2], phase separation [3], emulsion polymerisation [4] and spinning disk atomisation [5]. The most widely used route for manufacture still remains the emulsion-solvent evaporation technique [3].

A typical emulsion process involves dissolving a polymer in a volatile organic solvent and emulsifying this phase in an aqueous phase containing a surfactant to form an oil-in-water (O/W) emulsion, followed by solvent evaporation while stirring. By this emulsion process, typically, non-porous microparticles are obtained. However by controlling the solvent evaporation rate, for example, particles can be modified to be microporous [6]. To further increase the particles porosity, porogens such as sodium chloride and ammonium bicarbonate may be added [1,5]. The low density and high degree of porosity of the microparticles obtained by this technique makes them highly attractive for tissue engineering applications [1,5] and for pulmonary drug delivery [2]. In this study, we describe the fabrication of novel polycaprolactone microporous hemi-spherical microparticles called "hemi-shells" using a porogen-emulsion-solvent evaporation technique.

2. Experimental

2.1. Materials

Polycaprolactone (CAPA 6500, Mw 50000) was purchased from Solvay Chemicals (USA). Dichloromethane (DCM) and polyvinyl alcohol (PVA, average M_w 18000-23000, 87-89% hydrolyzed) were obtained from Sigma Aldrich (South Africa) and were of reagent grade and used as received. Glacial acetic acid (100%) and sodium bicarbonate ($NaHCO_3$) obtained from Merck (South Africa) were of analytical grade. $NaHCO_3$ was ground down and sieved into a narrow size range of 25-38µm before use.

2.2. Preparation of hemi-shells

Polycaprolactone hemi-shells were prepared by using an O/W technique. PCL (15% w/v) was fully dissolved in 10ml DCM (oil phase). $NaHCO_3$ (25-38µm) was then stirred into the oil phase with a porogen: PCL ratio of 2:1 by weight. PVA (1% w/v) was dissolved in 150ml deionized water (water phase). The O/W emulsion was prepared by using a Silverson homogenizer (Model L4RT, Silverson Machines, UK) at 300rpm for 2minutes at 25°C. The emulsion was solvent evaporated while constantly stirring at the same temperature. Glacial

acetic acid (2.4ml) was added after 30minutes to increase CO_2 gas evolution by the reaction (1) as given below:

$$NaHCO_3 + CH_3COOH \rightarrow CH_3COONa + H_2O + CO_2 \uparrow \quad \text{.....(1)}$$

After solvent evaporation was completed, the hemi-shells were isolated using filtration, washed three times with deionised water and the left to dry at 25℃.

2.3. Characterisation of hemi-shells

To monitor the morphological changes of the hemi-shells with time, small quantities were removed from the emulsion as solvent evaporation proceeded. These particles were examined using an optical microscope (Leica DME, USA) with a Leica DC 150 digital camera system. By using image analysis software (ImageJ, NIH), the number-average particle size and yield of hemi-shells were obtained with increasing time intervals (n = 200). Scanning electron microscopy (LEO 1525 field emission SEM with Oxford's INCA system) was used to observe the final hemi-shell morphology.

3. Results and discussion

Fig. 1 shows the morphological changes observed in the stages of hemi-shell development with time as observed using optical microscopy while still wet. After 10minutes of solvent-evaporation [Fig. 1a], the porogen dissolved forming small CO_2 gas bubbles which were entrapped within the polymeric microspheres. These bubbles gradually coalesced forming larger bubbles as seen at 20 and 30minutes [Fig. 1b,c]. It is hypothesized that these gas bubbles once fully coalesced [Fig. 2], eventually burst thus creating an internal cavity with an externally microporous shell as shown in the SEM micrograph [Fig. 1d].

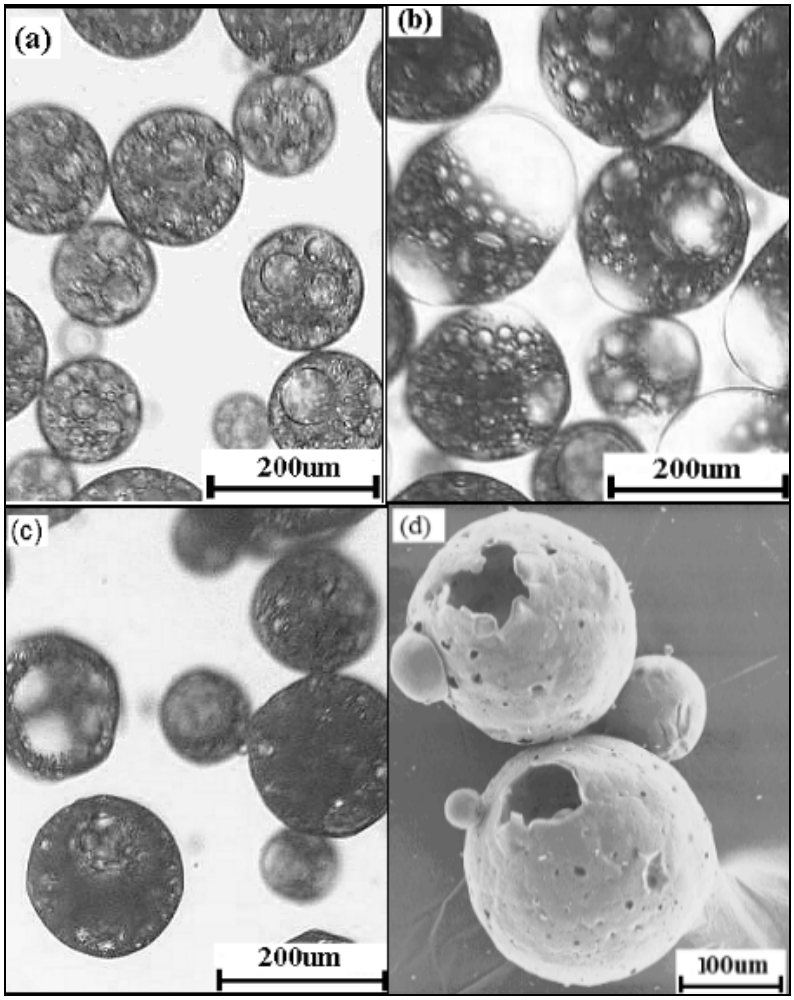

Fig. 1. Optical photomicrographs of the hemi-shell morphological development with time: (a) 10mins, (b) 20mins, (c) 30mins, and (d) SEM micrograph of the final morphology after solvent evaporation was completed

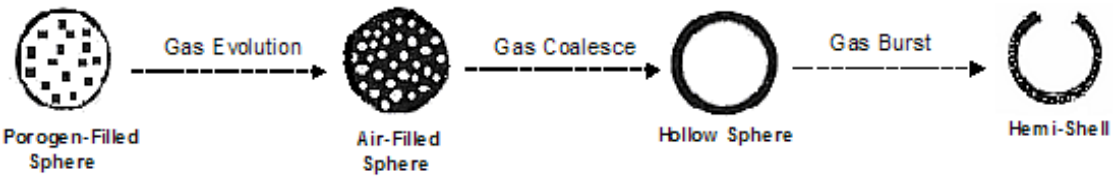

Fig. 2. Schematic of hemi-shell formation

Acid addition also increased the gas formation thus creating more porosity. Coalescence of smaller bubbles to form larger bubbles can be attributed to the change in Laplace pressure (2):

$$P_{inside} - P_{outside} = \frac{2\sigma}{r} \quad \text{.....(2)}$$

where $P_{inside,\ outside}$ is the internal and external pressure, respectively on the bubble, *r* is the bubble radius and σ is the surface tension. Gas evolution was also noted by Kim *et al* [1] in the formation of poly (lactic-co-glycolic acid) (PLGA) interconnected porous particles when using ammonium bicarbonate as a porogen in a water-in-oil-water (W/O/W) emulsion.

Fig. 3 illustrates the change in the number-average particle size and hemi-shell yield with solvent evaporation time. The number-average particle size decreased with time from 163µm to 149µm as solvent evaporation progressed from 10 to 75minutes. A particle yield of 84% was obtained in the 50-200µm range after solvent evaporation was completed. Particle size decrease corresponded to an increase in hemi-shell yield where a yield of 41% was achieved after 75minutes. The increase in hemi-shell yield as explained above is due to the increase in bubble coalescence as the polymeric microspheres shrink during solvent evaporation which is analogous to the coalescence seen in W/O/W emulsions [8]. Other morphologies, such as hollow particles, were also obtained by this emulsion method by changing variables such as the solvent evaporation rate, surfactant type etc.

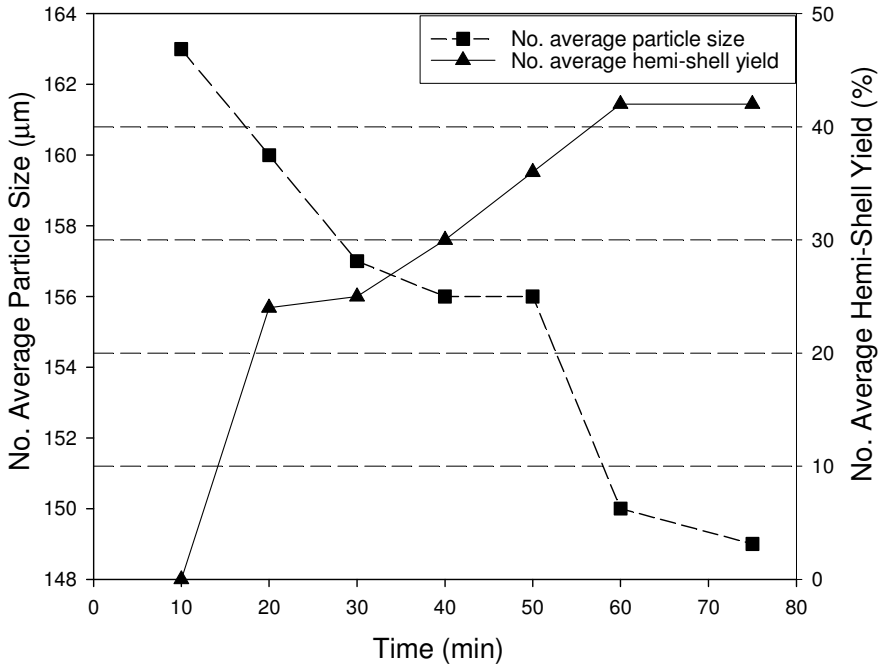

Fig. 3. Plot of change in number-averaged particle size and hemi-shell yield with solvent evaporation time

4. Conclusions

Novel microporous polycaprolactone hemi-shells with a number-average particle yield of 84% in the 50-200μm range have been successfully produced by sodium bicarbonate addition into a modified O/W emulsion. The gas evolution from porogen dissolution leads to a highly porous microparticle at the onset, which finally develops into a hollow concavity with a microporous shell. Hemi-shells displayed central openings of up to 75μm in diameter with surface micropores of 20μm in diameter. This unique morphology has potential applications in tissue engineering, and drug delivery amongst others.

References

[1] Kim TK, Yoon JJ, Lee DS, Park TG, Biomaterials 27 (2006) 152-159.
[2] Edwards DA, Hanes J, Langer R, Science 276 (1997) 1868-1871.
[3] Hong Y, Gao C, Shi Y, Shen J, Polym. Adv. Technol. 16 (2005) 622-627.
[4] Hong Z, Bo L, Guangsu H, Mater. Lett. 60 (2006) 3451-3456.
[5] Senuma Y, Franceshin S, Hilborn JG, Tissieres P, Bisson I, Frey P, Biomaterials 21 (2000) 1135-1144.
[6] Jeyanthi R, Thanoo BC, Metha RC, Deluca PD, J. Control. Rel. 38 (1996) 235-244.
[7] Ducker WA, Xu Z, Israelachvili JN, Langmuir 10 (1984) 3279-3289.
[8] Crotts G, Park TG, J. Control Rel. 35 (1995) 91-105.